

VIVA, VLA IMAGING OF VIRGO SPIRALS IN ATOMIC GAS:
I. THE ATLAS & THE HI PROPERTIES

AEREE CHUNG^{1,2}, J. H. VAN GORKOM¹, JEFFREY D. P. KENNEY³, HUGH CROWL^{3,4} AND BERND VOLLMER⁵
Accepted for publication in AJ

ABSTRACT

We present the result of a new VLA HI Imaging survey of Virgo galaxies, VIVA (the VLA Imaging survey of Virgo galaxies in Atomic gas). The survey includes high resolution HI data of 53 carefully selected late type galaxies (48 spirals and 5 irregular systems). The goal is to study environmental effects on HI gas properties of cluster galaxies to understand which physical mechanisms affect galaxy evolution in different density regions, and to establish how far out the impact of the cluster reaches. As a dynamically young cluster, Virgo contains examples of galaxies experiencing a variety of environmental effects. Its nearness allows us to study each galaxy in great detail. We have selected Virgo galaxies with a range of star formation properties in low to high density regions (at the projected distance from M87, $d_{87} = 0.3\text{--}3.3$ Mpc). Contrary to previous studies, more than half of the galaxies in the sample ($\sim 60\%$) are fainter than 12 mag in B_T . Overall, the selected galaxies represent the late type Virgo galaxies (S0/a to Sd/Irr) down to $m_p \lesssim 14.6$ fairly well in morphological type, systemic velocity, subcluster membership, HI mass and deficiency. The HI observations were done in CS configuration of the Very Large Array radio telescope, with a typical spatial resolution of $15''$ and a column density sensitivity of $\approx 3 - 5 \times 10^{19} \text{ cm}^{-2}$ in 3σ per 10 km s^{-1} channel. The survey was supplemented with data of comparable quality from the NRAO archive, taken in CS or C configuration. In this paper (VIVA I: the atlas and the HI properties), we present HI channel maps, total intensity maps, velocity fields, velocity dispersions, global/radial profiles, position-velocity diagrams and overlays of HI/1.4 GHz continuum maps on the optical images. We also present the HI properties such as total flux (S_{HI}), HI mass (M_{HI}), linewidths (W_{20} & W_{50}), velocity (V_{HI}), deficiency (def_{HI}), size ($D_{\text{HI}}^{\text{eff}}$ & $D_{\text{HI}}^{\text{iso}}$), and describe the HI morphology and kinematics of individual galaxies in detail. The survey has revealed details of HI features that were never seen before. In this paper we briefly discuss differences in typical HI morphology for galaxies in regions of different galaxy densities. We confirm that galaxies near the cluster core ($d_{87} \lesssim 0.5$ Mpc) have small HI disks compared to their stellar disks ($D_{\text{HI}}/D_{25} < 0.5$). Most of these galaxies in the core also show gas displaced from the disk, which is either currently being stripped, or falling back after a stripping event. At intermediate distances ($d_{87} \sim 1$ Mpc) from the center we find a remarkable number of galaxies with long one sided HI tails pointing away from M87. In a previous letter we argue that these are galaxies recent arrivals, falling in for the first time into the Virgo core. In the outskirts we find many gas-rich galaxies, with gas disks extending far beyond the optical. Interestingly we also find some galaxies with HI disks that are small compared to their stellar disk at large clustercentric distances.

Subject headings: galaxies: clusters — galaxies: evolution — galaxies: interactions — galaxies: kinematics and dynamics

1. INTRODUCTION

It has long been known that cluster galaxies appear to be different from field galaxies in their morphological type and color (e.g. Hubble & Humason 1931). In the local universe $\sim 90\%$ of the population in the core regions of rich clusters consists of ellipticals and S0's while spirals dominate in the field (Dressler 1980). This could

either mean that galaxies form differently in dense environment or that galaxies are affected by their surroundings. Many mechanisms could drive environmental evolution, for example ram-pressure stripping (Gunn & Gott 1972), turbulent/viscous stripping (Nulsen 1982), thermal evaporation (Cowie & Songaila 1977), starvation (Larson et al. 1980), interaction with the cluster potential (Bekki 1999), harassment, the cumulative effect of many fast interactions (Moore et al. 1996), slow interactions between individual galaxies (Mihos 2004) and mergers.

Single dish 21 cm observations, such as Davies & Lewis (1973), Chamaroux, Balkowski & Gerard (1980) and Giovanelli & Haynes (1985) have found that spirals near the cluster core regions are very deficient in their neutral atomic hydrogen gas, HI, compared to galaxies of the same morphological type and size in the field. Giovanelli & Haynes (1985) first showed that not only the gas content but also the size of the gas disks is affected. Subsequent HI imaging studies of nearby clus-

¹ Department of Astronomy, Columbia University, 550 West 120th Street, New York, NY 10027, U.S.A.; jvan-gork@astro.columbia.edu

² Currently NRAO Jansky Postdoctoral Fellow at the National Radio Astronomy Observatory, P.O. Box O, Socorro, NM 87801, U.S.A.; achung@aoc.nrao.edu

³ Department of Astronomy, Yale University, P.O. Box 208101, New Haven, CT 06520, U.S.A.; kenney@astro.yale.edu, hugh@astro.yale.edu

⁴ Current address: Department of Astronomy, University of Massachusetts, 710 North Pleasant Street, Amherst, MA 01003-9305, USA; hugh@astro.umass.edu

⁵ Observatoire astronomique de Strasbourg, 11 rue de l'universite, 67000 Strasbourg, France; bvollmer@astro.u-strasbg.fr

ters like Virgo and Coma (Warmels 1988a; Cayatte et al. 1990; Bravo-Alfaro et al. 2000), showed that the HI disks of the highly HI deficient galaxies are severely truncated to within the stellar disk. These images of unperturbed stellar disks with highly truncated gas disks strongly suggest that galaxies lose their interstellar gas (ISM) through an interaction with the hot intracluster medium (ICM).

However, there are still remaining questions. First, Dressler (1980) already pointed out that ram pressure stripping by the hot ICM alone cannot be responsible for the transformation of spirals into S0's. The morphology density relation changes very smoothly and a significant fraction of S0's reside in low density environment, and the bulge to disk ratios of S0's are systematically larger in all density regimes. This cannot be caused by a simple ISM stripping. More recently, in a study of 18 nearby clusters, Solanes et al. (2001) show that the HI deficiency decreases gradually with increasing projected distance from the cluster center out to ~ 2 Abell radii ($\approx 3h^{-1}$ Mpc). A similar trend is found in star formation rate which begins to decrease at a clustercentric radius of 3-4 virial radii or 1.5 Abell radii (e.g. Lewis et al. 2002; Gómez et al. 2003). These results suggest that galaxies are already modified in much lower density environments, where ram pressure is expected to be unimportant, and now the question has become: how exactly are galaxies affected in different density regions? That is, how far out do galaxies feel the impact of the cluster, which mechanisms are at work in lower density environments, and what are the dominant environmental effects onto disks that galaxies experience as they come close to the cluster center?

In order to answer these questions, we have probed the cluster environment using high resolution HI data on a sample of carefully selected Virgo galaxies. The HI gas is often a good tracer of different physical processes as it gets affected both by the intracluster medium (ICM) and gravitational interactions. Also, the outer gas disk is mostly in atomic form, where it is more vulnerable to the surroundings. In addition, it provides useful diagnostics for galaxy evolution as it is the fuel for star formation. The HI data were taken using the Very Large Array (VLA)⁶. The VLA has had significant improvements since the previous Virgo survey. The L band (20 cm) receivers have been replaced and the C array has been replaced by the C short (CS) configuration. Our high resolution, high sensitivity VLA HI data allow us to investigate not only the evolutionary history of individual galaxies but also the overall impact of Virgo on its members.

Several results of the survey and a preceding pilot for the survey have already been published. Kenney, van Gorkom & Vollmer (2004), and Vollmer et al. (2004b) present an analysis of the data on NGC 4522, a galaxy far away from M87, yet stripped to well within the optical disk and showing abundant evidence for currently ongoing stripping. They suggest that NGC 4522 possibly shows evidence for enhanced ram pressure due to

bulk motions or substructure of the ICM. Crowl et al. (2005) present HI, radio continuum and high quality optical images of the edge-on galaxy NGC 4402, which shows evidence for dense cloud ablation. One of the striking results of the survey is a number of one sided long HI tails pointing away from the cluster center and at intermediate distances from M87. Chung et al. (2007) argue that these are probably galaxies recently arrived near the cluster and falling into the cluster for the first time. Some of our data have already been used to constrain simulations of individual systems, for example on NGC 4522 (Vollmer et al. 2006) and NGC 4501 (Vollmer et al. 2008).

In this work, we present the complete HI atlas and describe the HI properties of individual galaxies in detail. In a second paper we will present a statistical analysis of our results and discuss the impact of the different environmental effects.

This paper is organized as follows. In § 2 we describe our selection criteria and present the general properties of the sample. In § 3 we present the observations and data reduction. In § 4 we describe the HI atlas, which is appended at the end. In § 5 we measure the HI quantities such as mass, linewidth, velocity, deficiency, and size, and compare our HI fluxes with values found in the literature. We then present our main findings on the HI morphology in § 6, followed by a summary of the main results in § 7. In an appendix we present the full HI atlas and comment on individual galaxies. Throughout this paper we assume that the distance to Virgo is 16 Mpc (Yasuda et al. 1997).

2. SAMPLE

2.1. The Virgo Cluster

Virgo is the nearest rich galaxy cluster. Binggeli, Sandage & Tammann (1985) have cataloged 2096 galaxies (VCC, Virgo Cluster Catalog) in ~ 140 deg² area centered on $\alpha, \delta_{1950} = 12^{\text{h}}25^{\text{m}}, 13^{\circ}$ (~ 1 degree northwest of M87). About 1300 galaxies have been identified as true members based on the morphological appearance and the measured radial velocities. The X-ray emission from the hot cluster gas (Böhringer et al. 1994) shows plenty of substructures, indicating that Virgo is far from being virialized but still growing as several subclusters (the M86 and M49 group) merge into the main cluster around M87. The velocities and the surface brightness fluctuation (SBF) distances of M87, M86 and M49, which are noted in black in Figure 1, are 1307, -244 and 997 km s⁻¹ (Smith et al. 2000), and 16.1, 18.4 (West & Blakeslee 2000) and 16.3 Mpc (Ferrarese et al. 2003), respectively. The M86 group is falling in from the back and M49 is likely to be merging with the M87 group, falling in from the south in the plane of the sky (Tully & Shaya 1984; Schindler et al. 1999). For more detailed discussions of the 3-dimensional structure of the Virgo cluster, see for example Gavazzi et al. (1999) and Mei et al. (2007).

Since Virgo is nearby, it is an ideal target for HI imaging studies, and two major imaging surveys were done in the past. Warmels (1988a) and Cayatte et al. (1990) have mapped 15 and 25 bright Virgo spirals with the Westerbork Synthesis Radio Telescope (WSRT) and the VLA respectively. Those studies have shown that the HI disks of the central galaxies are truncated to well within the optical disks, making it likely that ICM-ISM interac-

⁶ The VLA is operated by the National Radio Astronomy Observatory, which is a facility of the National Science Foundation (NSF), operated under cooperative agreement by Associated Universities, Inc.

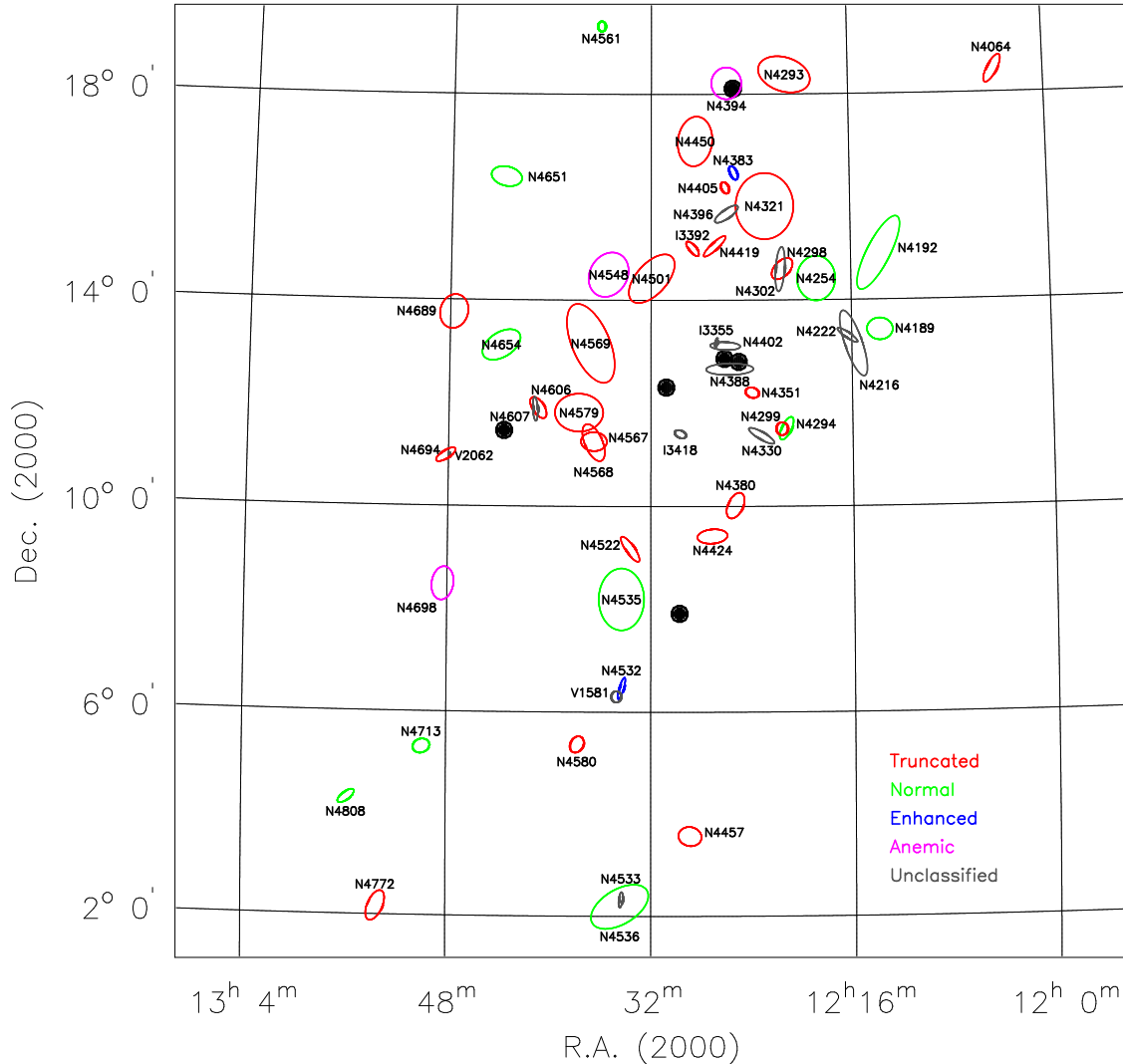


FIG. 1.— The VIVA galaxies are shown at their proper positions with NGC (N), IC (I) or VCC (V) names. Each galaxy is indicated by an ellipse which represents $D_{25} \times 10$ and is drawn using the position angle and the inclination measured in the optical B -band. Galaxies are color-coded based on the star formation properties classified in the $H\alpha$ study by Koopmann & Kenney (2004b), except for light grey which indicates the ones not included in the sample of Koopmann & Kenney (2004a, b). Six big ellipticals are shown in large black dots (M85, M86, M84, M87, M60 and M49 in order of decreasing declination).

tions are at least partly responsible for driving the evolution of galaxies in the cluster inner region. Here we present the results of a new survey that includes twice as many galaxies, covers a much wider range in galaxy mass and probes the lower density outer regions as well as the high density core.

2.2. VIVA Sample

Koopmann & Kenney (2004a) studied the $H\alpha$ morphology of 84 Virgo galaxies, including fainter spirals which were never extensively studied. Using R -band and $H\alpha$ surface brightness profiles, Koopmann & Kenney (2004b) classified the star formation properties of these 52 Virgo galaxies into several categories; normal, anemic, enhanced, and truncated. They argue that these categories are likely to reflect different evolutionary phases and different types of interactions with the cluster environment. Since we wanted to sample galaxies undergoing different environmental effects we have selected 46

Virgo galaxies showing a range of star formation properties based on Koopmann & Kenney (2004b)'s classification.

The survey also probes both the high and the low density regions, covering angular distances of $\sim 1^\circ - 12^\circ$ from M87. At the distance of 16 Mpc this corresponds to 0.3-3.3 Mpc. Thus we probe galaxies out to a distance of ~ 1.6 Abell radii ($r_A \sim 1.5 h^{-1}$ Mpc and $H_0 = 71 \text{ km s}^{-1} \text{ Mpc}^{-1}$; Spergel et al. 2003) or 4 virial radii ($r_{vir} \sim 0.8$ Mpc for Virgo; Tully & Shaya 1984).

In addition we selected two galaxies that are not in the Koopmann & Kenney (2004a, b) sample. These two galaxies, NGC 4330 and IC 3418, show morphological peculiarities in the UV (the GALEX nearby galaxy survey). NGC 4330 is a highly inclined disk galaxy and has a warped UV tail extending beyond the optical disk on one side. IC 3418 is optically a low surface brightness system, which shows in UV a displacement from the optical disk with an extended broad UV tail on one side.

TABLE 1
VIVA SAMPLE AND GENERAL PROPERTIES

(1)	(2)	(3)		(4)	(5)	(6)	(7)	(8)	(9)	(10)	(11)	(12)
Galaxy	VCC	α_{2000}	δ_{2000}	Type	D_{25}	B_T	PA	i	V	d_{M87}	SF	
		<i>hhmmss.s</i>	<i>ddmmss</i>		$''$	mag	$^\circ$	$^\circ$	km s^{-1}	deg		
NGC 4064	...	12 04 10.8	+18 26 34	SB(s)a: pec	4.37	12.22	150	69	1000	9.0	T/C	
NGC 4189	89	12 13 46.8	+13 25 36	SAB(rs)cd	2.40	12.51	66 ^c	45	1995	4.4	N	
NGC 4192	92	12 13 48.2	+14 53 43	SAB(s)ab	9.77	10.95	155	78	-126	4.9	N	
NGC 4216	167	12 15 53.1	+13 08 58	SAB(s)b	8.13	10.99	19	85	30	3.8	...	
NGC 4222*	187	12 16 22.7	+13 18 31	Sd	3.31	13.86	56	90	225	3.7	...	
NGC 4254	307	12 18 49.4	+14 25 07	SA(s)c	5.37	10.44	68 ^c	30	2453	3.6	N	
NGC 4293	460	12 21 13.0	+18 22 58	(R)SB(s)0	5.62	11.26	72	65	717	6.5	T/A	
NGC 4294	465	12 21 17.4	+11 30 40	SB(s)cd	3.24	12.53	155	70	421	2.5	N	
NGC 4298	483	12 21 32.7	+14 36 25	SA(rs)c	3.24	12.04	140	57	1122	3.2	T/N	
NGC 4299	491	12 21 40.6	+11 30 15	SAB(s)dm	1.74	12.88	42 ^c	22	209	2.5	T/E	
NGC 4302	497	12 21 42.5	+14 36 05	Sc	5.50	12.50	178	90	1111	3.2	...	
NGC 4321	596	12 22 55.2	+15 49 23	SAB(s)bc	7.41	10.05	30	33	1579	4.0	T/N	
NGC 4330	630	12 23 16.5	+11 22 06	Scd?	4.47	13.09	59	90	1567	2.1	*	
NGC 4351	692	12 24 01.8	+12 12 24	SB(rs)ab: pec	1.20	13.03	61 ^c	49	2388	1.7	T/N	
NGC 4380	792	12 25 22.2	+10 00 57	SA(rs)b	3.47	12.66	153	58	935	2.7	T/A	
NGC 4383	801	12 25 25.6	+16 28 12	Sa: pec	1.95	12.67	13 ^c	60	1663	4.3	E	
NGC 4388	836	12 25 47.0	+12 39 42	SA(s)b	5.62	11.76	92	83	2538	1.3	...	
NGC 4394	857	12 25 56.1	+18 12 54	(RS)B(r)b	3.63	11.73	113 ^c	28	772	5.9	A	
NGC 4396	865	12 25 59.3	+15 40 19	SAd	3.31	13.06	125	77	-133	3.5	...	
NGC 4405	874	12 26 07.5	+16 10 50	SA(rs)0	1.78	13.03	20	51	1751	4.0	T/N	
NGC 4402	873	12 26 07.9	+13 06 46	Sb	3.89	12.55	90	78	190	1.4	...	
IC 3355*	945	12 26 50.0	+13 10 36	Im	1.12	15.18	172	68	127	1.3	...	
NGC 4419	958	12 26 56.9	+15 02 52	SB(s)a	3.31	12.08	133	74	-224	2.8	T/A	
NGC 4424	979	12 27 11.5	+09 25 15	SB(s)a	3.63	12.34	95	62	447	3.1	T/C	
NGC 4450	1110	12 28 29.4	+17 05 05	SA(s)ab	5.25	10.90	175	43	2048	4.7	T/A	
IC 3392	1126	12 28 43.7	+15 00 05	SAb	2.29	12.99	40	67	1678	2.7	T/A	
NGC 4457	1145	12 28 59.3	+03 34 16	(R)SAB(s)0	2.69	11.76	82 ^c	33	738	8.8	T/N	
IC 3418	1217	12 29 43.5	+11 24 08	IBm	1.48	14.00	...	50	38	1.0	*	
NGC 4501	1401	12 31 59.6	+14 25 17	SA(rs)b	6.92	10.36	140	59	2120	2.1	T/N	
NGC 4522	1516	12 33 40.0	+09 10 30	SB(s)cd	3.72	12.99	33	79	2332	3.3	T/N	
NGC 4532	1554	12 34 19.4	+06 28 12	IBm	2.82	12.30	160	70	2154	6.0	E	
NGC 4535	1555	12 34 20.3	+08 11 53	SAB(s)c	7.08	10.59	0	46	1973	4.3	N	
NGC 4533*	1557	12 34 22.2	+02 19 31	SAd	2.09	14.20	161	88	1753	10.1	...	
NGC 4536	1562	12 34 26.9	+02 11 19	SAB(rs)bc	7.59	11.16	130	67	1894	10.2	N	
HolmbergVII* ^a	1581	12 34 44.8	+06 18 10	Im	1.29	14.62	82 ^c	22	2039	6.2	...	
NGC 4548	1615	12 35 26.3	+14 29 49	SB(rs)b	5.37	10.96	150	38	498	2.4	A	
NGC 4561	...	12 36 08.6	+19 19 26	SB(rs)dm	1.51	12.90	30	33	1441	7.1	N	
NGC 4567	1673	12 36 32.8	+11 15 31	SA(rs)bc	2.95	12.06	85	49	2213	1.8	T/N	
NGC 4568	1676	12 36 34.7	+11 14 15	SA(rs)bc	4.57	11.68	23	66	2260	1.8	T/N	
NGC 4569	1690	12 36 50.1	+13 09 48	SAB(rs)ab	9.55	10.26	23	65	-311	1.7	T/N	
NGC 4579	1727	12 37 44.2	+11 49 11	SAB(rs)b	5.89	10.48	95	38	1627	1.8	T/N	
NGC 4580	1730	12 37 48.4	+05 22 09	SAB(rs)a: pec	2.09	11.83	165	40	1227	7.2	T/N	
NGC 4606	1859	12 40 57.8	+11 54 41	SB(s)a	3.24	12.67	33	62	1653	2.6	T/C	
NGC 4607	1868	12 41 12.2	+11 53 09	SBb	2.88	13.75	2	83	2284	2.6	...	
NGC 4651	...	12 43 42.6	+16 23 40	SA(rs)c	3.98	11.39	80	50	788	5.1	N	
NGC 4654	1987	12 43 56.6	+13 07 33	SAB(rs)cd	4.90	11.10	128	56	1035	3.4	N	
NGC 4689	2058	12 47 45.8	+13 45 51	SA(rs)bc	4.27	11.60	161 ^c	37	1522	4.5	T/N	
VCC 2062* ^b	2062	12 47 59.9	+10 58 33	dE	0.69	19.00	42 ^c	7	1170	4.5	...	
NGC 4694	2066	12 48 15.1	+10 59 07	SB0: pec	3.16	12.06	140	63	1211	4.6	T/N	
NGC 4698	2070	12 48 23.5	+08 29 16	SA(s)ab	3.98	11.46	170	53	1032	5.9	A	
NGC 4713	...	12 49 58.1	+05 18 39	SAB(rs)d	2.69	12.19	100	52	631	8.5	N	
NGC 4772	...	12 53 29.1	+02 10 11	SA(s)a	3.39	11.96	147	62	1042	11.7	T/N	
NGC 4808	...	12 55 49.6	+04 18 14	SA(s)cd	2.75	12.35	127	68	738	10.2	N	

The data have been taken from *The Third reference catalogue of bright galaxies* (RC3; Phys. Rev. C3) unless noted. (1) First names as they appear in RC3. *Five bonus galaxies from the same field as the selected sample; (2) Virgo Cluster Catalog (VCC) number (Binggeli et al. 1985); (3) Right ascension in J2000; (4) Declination in J2000; (5) Morphological type; (6) Optical size of major axis measured at 25 mag \square''^{-1} in *B*-band; (7) Position angle; (8) Inclination derived from the ratio of major to minor axis, using the Hubble formula for oblate spheroids and an intrinsic axis ratio of 0.2, $i = \cos^{-1} \sqrt{1.024 b^2/a^2 - 0.042}$ (Aaronson et al. 1980); (9) Optical velocity; (10) Projected distance from M87; (11) Star formation property classified based on $H\alpha$ surface profiles (Koopmann & Kenney 2004b): N-normal, T-truncated, C-compact, E-enhanced, and A-anemic. *Galaxies not included in the sample of Koopmann & Kenney (2004b) but selected for the VIVA survey due to the morphological peculiarities in the *UV* wavelength; ^aIt will be referred with its VCC number (VCC 1581) hereafter; ^bThe data were taken from Binggeli et al. (1985) since it is not available from RC3. ^cPA's determined by us using the HI kinematics.

Lastly we have included five galaxies that were found in the HI data cubes of our targets, i.e. they are spatially and in velocity close to the target galaxies, bringing the total number of galaxies in the VIVA sample to 53.

In Figure 1, we show the locations of 53 selected galaxies. The different colors represent different star formation properties. In Figure 2, the optical and the *UV* images of the two galaxies that were not studied by Koopmann & Kenney (2004a, b) are shown. The general properties of the 53 galaxies are summarized in Ta-

ble 1. Note that more than half of the VIVA sample is fainter than 12 mag in B_T . Fainter galaxies appear to be more disturbed in $H\alpha$ and may be more vulnerable to environmental effects than more massive systems.

The VIVA sample probes the full range of the Virgo late type galaxy population. In Figure 3, we compare the general properties of the VIVA sample to those of a sample of 165 late-type (Sa-Im-BCD) Virgo galaxies that is complete to $m_p \leq 14.6$. The comparison sample is selected from a larger sample of 355 late-type Virgo

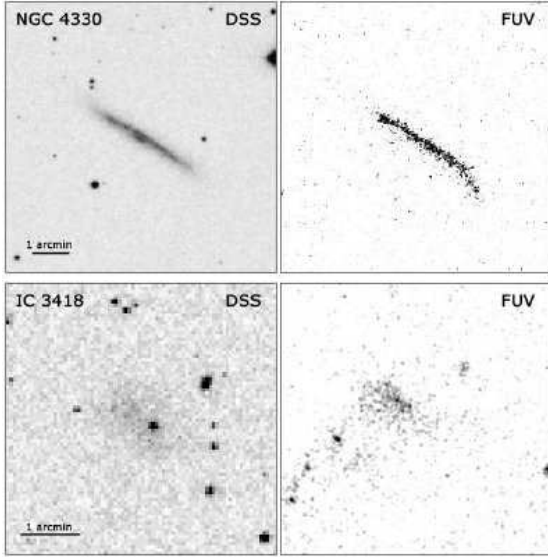


FIG. 2.— Two galaxies, NGC 4330 and IC 3418, have been selected based on the peculiarities in the *UV*. The Digitized Sky Survey (DSS) image is shown on the left and the GALEX image at far ultra-violet wavelength ($\lambda_{\text{center}} = 1530 \text{ \AA}$) is shown on the right. Note that NGC 4330 has the *UV* tail to the southwest where we do not find an optical counterpart. The *UV* emission of IC 3418 is displaced from the optical center and also shows a long *UV* stream ($> 2'$) to the southeast.

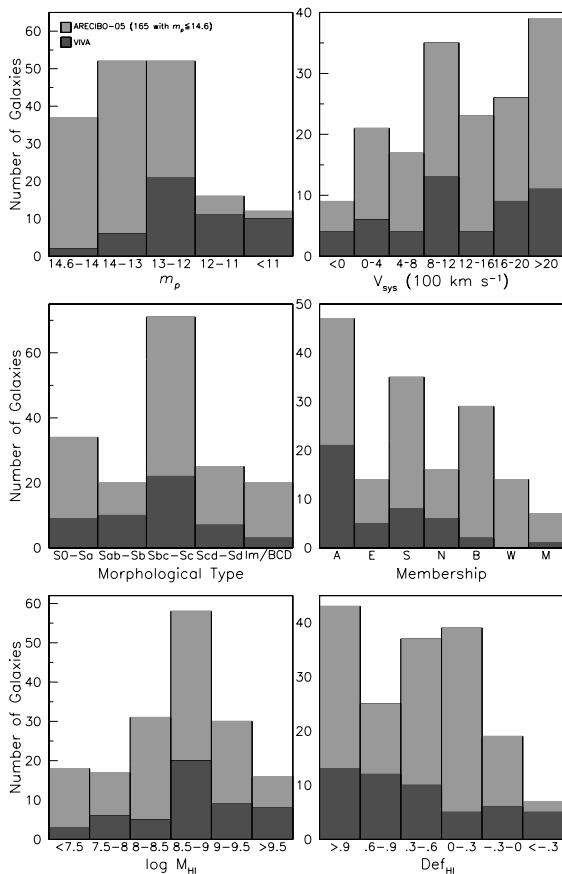


FIG. 3.— The statistics of the global properties of the VIVA sample compared to the ARECIBO-05 sample (Gavazzi et al. 2005). The VIVA sample of 53 galaxies is fairly representative for the late-type Virgo galaxies down to $m_p \approx 14.6$ in morphological type, velocity distribution and HI properties. Almost all of the selected galaxies are likely to be true members of the cluster.

galaxies, which is complete to $m_p \leq 18.0$ (Gavazzi et al. 2005). We have observed 32% of the galaxies in the complete sample of late type galaxies brighter than $m_p = 14.6$ (Gavazzi et al. 2005, ARECIBO-05 hereafter), including 75% of the galaxies with $m_p \leq 12$, 40% of the galaxies with $m_p = 12 - 13$ and eight galaxies which are fainter than $m_p > 13$. We have good coverage over all velocity bins, and all morphological types S0/a-Sd. Based on the subcluster membership classification by Gavazzi et al. (1999), all but 3 of the selected galaxies belong to the A, E, S and N subclusters, and are likely to be true members of the cluster. Based on an $H\alpha$ rotation curve and the H-band Tully Fisher relation Gavazzi et al. (1999) find that NGC 4380 might belong to the B cloud which is located at 23 Mpc. The distances to NGC 4424 and NGC 4189 are highly uncertain, but note that Cortés et al. (2008) using a stellar kinematics based Tully-Fisher distance find that NGC 4424 does belong to the Virgo Cluster. It remains true that distances to some of the individual galaxies in Virgo are controversial (Yasuda et al. 1997; Solanes et al. 2002). The VIVA sample also covers a wide range of HI mass and deficiency.

3. OBSERVATIONS & DATA REDUCTION

3.1. Observations

Since the previous VLA Virgo survey by Cayatte et al. (1990), several improvements have been made to the VLA. In 1998 the C array was replaced by the CS (C short) array by putting one antenna in the center of the array. This means that CS and D array now have the same shortest spacing. Compared to the C array the CS array has much better short spacing baseline coverage while the longer spacings are unchanged with spacings ranging from 0.035 to 3.4 km. Hence the CS array has better surface brightness sensitivity than the former C array, and the same angular resolution. In addition new L-band receivers have been installed, which have a much lower system temperature.

All the new observations were done with the VLA in CS array, in a few cases supplemented by D array. Most galaxies were observed with 3.125 MHz bandwidth. The correlator was configured to produce 127 channels and two polarizations. Online Hanning smoothing was applied after which every other channel was discarded. This resulted in 63 independent channels with a velocity resolution of roughly 10 km s^{-1} . Two galaxies, NGC 4606 and NGC 4607, were observed in one pointing. Since their velocities differ by 600 km s^{-1} a total bandwidth of 6.25 MHz was used, two polarizations and no online Hanning smoothing, resulting in 63 channels with 21 km s^{-1} width. In addition to these new observations we reprocessed archival data on Virgo galaxies that were of comparable quality, taken in C or CS array, including nine galaxies that were observed by us earlier. We have reached a column density sensitivity of $3\text{--}5 \times 10^{19} \text{ cm}^{-2}$ in 3σ per channel with a typical spatial resolution of $15\text{--}16''$ ($\lesssim 1.1 \text{ kpc}$ at the Virgo distance). This is a factor 3 and 4 better in spatial and spectral resolution respectively than the data of the previous VLA survey by Cayatte et al. (1990).

For some galaxies we suspected that we were missing extended diffuse emission based on the images or based on a comparison with single dish measurements. For those galaxies we either obtained D array data our-

TABLE 2
VIVA SURVEY OBSERVATIONAL PARAMETERS

(1)	(2)	(3)	(4)	(5)	(6)	(7)	(8)	(9)	(10)
Galaxy	Conf.	α, δ_{2000} h m s + ° ' ''	Obs. Date mon-yr	Int. hr	ΔB MHz	v_{obs} km s ⁻¹	Beam (PA) '' × '' (deg)	rms mJy beam ⁻¹	Ref.
N4064	CS	12 04 11.2+18 26 36	Mar04	8	3.125	930	16.28 × 16.14 (-79)	0.29	
N4189	CS	12 13 47.2+13 25 29	Apr04	8	3.125	2113	16.49 × 15.55 (+33)	0.32	
N4192	C/D	12 13 48.1+14 53 46	Jan91/May92	3/2.5	3.125	-160	27.99 × 25.90 (+76)	1.00	
N4216	C	12 15 53.7+13 08 42	Jan91	4.5	3.125	120	16.44 × 15.90 (-33)	0.65	
N4222	C	12 16 22.5+13 18 25	Jan91	4.5	3.125	120	16.44 × 15.90 (-33)	0.54	
N4254	C/D	12 18 49.3+14 25 07	Mar92/Apr91	8	3.125	2408	26.78 × 24.46 (+48)	0.41	Phookun et al. (1993)
N4293	CS	12 21 12.9+18 22 57	Jul05	8	3.125	893	16.58 × 15.40 (-69)	0.33	
N4294	CS/D	12 21 17.8+11 30 40	Apr04/Nov05,Jan06	8/3.5	3.125	293	28.93 × 26.74 (-34)	0.29	
N4298	CS	12 21 32.8+14 36 22	Jul05	8	3.125	1142	16.85 × 15.72 (-59)	0.35	
N4299	CS/D	12 21 40.5+11 30 11	Apr04/Nov05,Jan06	8/3.5	3.125	293	28.93 × 26.74 (-34)	0.29	
N4302	CS	12 21 42.5+14 35 52	Jul05	8	3.125	1142	16.85 × 15.72 (-59)	0.35	
N4321	CS/D	12 22 54.8+15 49 21	Mar04/Mar03	8/2.3	2.629	1571	31.10 × 28.11 (-26)	0.37	
N4330	CS/D	12 23 17.2+11 22 05	Aug05/Dec05	8	3.125	1565	26.36 × 23.98 (-56)	0.38	
N4351	CS	12 24 01.6+12 12 18	Feb04	8	3.125	2315	16.77 × 16.31 (-38)	0.30	
N4380	CS	12 25 22.1+10 01 01	Aug05	8	3.125	967	16.53 × 15.51 (-47)	0.37	
N4383	CS/D	12 25 25.5+16 28 12	Mar04/Dec05	8	3.125	1710	44.58 × 37.81 (-38)	0.26	
N4388	CS	12 25 46.6+12 39 44	Nov02	8	3.125	2524	17.14 × 15.12 (+01)	0.36	
N4394	CS	12 25 55.6+18 12 50	Jul05	8	3.125	922	16.71 × 15.17 (-59)	0.32	
N4396	CS/D	12 25 58.8+15 40 17	Mar04	8	3.125	-128	27.39 × 26.84 (-03)	0.28	
N4405	CS	12 26 07.0+16 10 51	Jul05	8	3.125	1747	16.59 × 15.36 (-61)	0.36	
N4402	CS	12 26 07.8+13 06 43	Jan03	8	3.125	200	17.07 × 15.27 (+07)	0.33	Crowl et al. (2005)
I3355	CS	12 26 51.1+13 10 33	Jan03	8	3.125	200	17.07 × 15.27 (+07)	0.36	
N4419	CS	12 26 56.4+15 02 50	Oct02	8	3.125	-261	16.35 × 15.26 (-09)	0.32	
N4424	CS	12 27 11.5+09 25 14	Apr04	8	3.125	439	17.59 × 15.53 (+36)	0.39	
N4450	CS	12 28 29.5+17 05 06	Jul05	8	3.125	1954	16.45 × 15.61 (-79)	0.36	
I3392	CS	12 28 43.3+14 59 58	Oct02	8	3.125	1687	17.06 × 15.06 (+15)	0.28	
N4457	CS	12 28 58.9+03 34 14	Jul05	8	3.125	882	17.43 × 16.28 (-36)	0.47	
I3418	CS	12 29 43.8+11 24 09	Aug05	8	3.125	38*	16.67 × 15.77 (-64)	0.43	
N4501	C	12 31 59.0+14 25 10	Jan91	5	3.125	2280	16.99 × 16.56 (+51)	0.57	
N4522	CS	12 33 39.7+09 10 31	Mar00	8	3.125	2330	18.88 × 15.20 (-43)	0.40	Kenney et al. (2004)
N4532	C	12 34 19.3+06 28 04	Dec94	5.5	3.125	2000	17.36 × 16.19 (+22)	0.33	Hoffman et al. (1999)
N4535	C/D	12 34 20.3+08 12 01	Jan91/Jan94	5	3.125	1950	24.98 × 24.07 (+22)	0.60	
N4533	CS	12 34 22.0+02 19 31	Mar04	8	3.125	1790	18.04 × 16.18 (-12)	0.33	
N4536	CS	12 34 27.0+02 11 17	Mar04	8	3.125	1790	18.04 × 16.18 (-12)	0.33	
V1581	C	12 34 45.3+06 18 02	Dec94	5.5	3.125	2000	17.36 × 16.19 (+22)	0.33	Hoffman et al. (1999)
N4548	CS	12 35 26.4+14 29 47	Mar04	5	3.125	451	16.59 × 15.81 (-37)	0.30	
N4561	C	12 36 08.5+19 19 25	Sep89	3	3.125	1400	15.44 × 14.00 (-39)	1.40	
N4567	CS	12 36 32.7+11 15 28	Jul05	8	3.125	2265	17.12 × 15.98 (-53)	0.36	
N4568	CS	12 36 34.3+11 14 19	Jul05	8	3.125	2265	17.12 × 15.98 (-53)	0.36	
N4569	CS	12 36 49.8+13 09 46	Apr04	8	3.125	-235	16.38 × 16.27 (+10)	0.33	
N4579	CS/D	12 37 43.3+11 49 05	Feb04/Mar03	8/2.3	2.629	1519	42.42 × 34.49 (+37)	0.45	
N4580	CS	12 37 48.4+05 22 10	May04	8	3.125	1036	17.37 × 16.34 (-03)	0.31	
N4606	CS	12 40 57.6+11 54 40	Aug05	8	6.25	1961	16.68 × 15.49 (-54)	0.29	
N4607	CS	12 41 12.4+11 53 09	Aug05	8	6.25	1961	16.68 × 15.49 (-54)	0.29	
N4651	CS	12 43 42.6+16 23 36	Mar04	8	3.125	804	16.67 × 16.25 (-69)	0.40	
N4654	C	12 43 56.5+13 07 33	Mar92	8	3.125	1088	16.14 × 15.52 (+35)	0.45	Phookun & Mundy (1995)
N4689	CS	12 47 45.5+13 45 46	Mar04	8	3.125	1611	16.71 × 15.85 (-37)	0.27	
V2062	CS	12 47 59.9+10 58 33	May04	8	3.125	1117	16.35 × 16.12 (+12)	0.38	
N4694	CS	12 48 15.1+10 58 58	May04	8	3.125	1117	16.35 × 16.12 (+12)	0.38	
N4698	CS	12 48 22.9+08 29 14	Apr04	8	3.125	1000	16.96 × 16.20 (-29)	0.35	
N4713	C	12 49 58.0+05 18 38	Sep89	2	3.125	655	25.95 × 22.13 (+67)	1.96	
N4772	CS	12 53 29.1+02 10 06	Jul05	8	3.125	1040	17.80 × 15.41 (-36)	0.36	
N4808	C/D	12 55 49.5+04 18 14	Sep89/Nov05	2	3.125	760	40.01 × 35.53 (+08)	0.59	

Footnote for Table 2: (1) NGC, IC or VCC names; (2) VLA configuration(s); (3) Field center; (4) Observation dates in month and year; (5) Observation duration; (6) Total bandwidth. Note that NGC 4321 and NGC 4579 were observed in the way that two 3.125-IF's were offset with each other with 14 channels overlapping around the velocity where the observations were centered at, resulting in the total bandwidth of 2.629 MHz; (7) Heliocentric velocity of the central channel using optical definition; (8) Synthesized beam FWHM (PA of the beam); (9) The rms per channel of the final cube imaged with robust=1; (10) The literature where the same data have been presented.

selves or we used archival data of comparable quality. For eleven galaxies in total we use the combined C/CS and D array data. Observing parameters are summarized in Table 2.

3.2. Data Reduction

Both the new and the archival data were reduced in the same way using the Astronomical Imaging Processing System (AIPS). After flux, phase and bandpass calibration, the continuum was subtracted by making a linear fit to the uv data for a range of line-free channels at both sides of the band. High uv points caused by interference were flagged after continuum subtraction. Two galaxies (NGC 4321 and NGC 4579) were observed with

overlapping IFs, which were offset by ~ 120 km s⁻¹. For those two galaxies we converted the two IFs into one long spectrum by averaging the overlapping channels, using UJOIN. Several channels at both edges of the IFs, where the spectral frequency response drops rather steeply, were not included.

First we made low resolution cubes covering a large field of view (1.4×1.4 deg²) to search for HI emission of sources far away from the field center. We found five galaxies that were fully covered in velocity and we added those to the VIVA survey (see §2.2 and Table 1).

The final image cubes were made using ROBUST=1 (Briggs 1995) to maximize sensitivity while keeping good spatial resolution. The cubes were cleaned to remove the

sidelobes. The final cubes were about 40 arcmin in size, slightly larger than the FWHP (30 arcmin) of the primary beam of the VLA.

All but IC 3418 were previously detected with single-dish. In our survey IC 3418 is also the only target that was not detected in HI, down to $\sim 8 \times 10^6 M_\odot$ per beam in 3σ , assuming a profile width of 100 km s^{-1} . However, our sensitivity would be less to a huge/diffuse HI disk, which would be smooth over 10 arcminutes in a single velocity channel.

The total HI image, the intensity weighted velocity field and the velocity dispersion image were also produced using AIPS by taking moments along the frequency axis (0th, 1st and 2nd moments). The AIPS task MOMNT allows you to create a mask to blank the images at a given cutoff level. In creating a mask, we applied Gaussian and Hanning smoothing in spatial and in velocity, respectively, to maximize the signal-to-noise. We normally used $1 \sim 2 \times \text{rms}$ of the cube as the cutoff. We applied those masks to the full resolution cubes and calculated moments on the full resolution blanked cubes. Once image cubes and moment maps were obtained, we performed further analysis using the Groningen Image Processing SYstem (GIPSY).

We also made 1.4 GHz continuum images by averaging the line free channels. In order to reduce the effects of interfering sources, which may cause substantial sidelobes especially at low frequencies, we have used the AIPS task PEELR. It iteratively attempts to calibrate on multi fields around bright continuum sources (self-calibration), subtract the sources in those fields from the self-calibrated data, undo the field-specific calibration from the residual data, and it finally restores all fields to the residual data. We used the same weighting scheme (ROBUST=1) as for the HI images. The quality of our continuum data varies depending on the number of line free channels of individual target galaxies.

4. HI ATLAS: DESCRIPTIONS

In this section, we describe the atlas which is appended at the end. Individual galaxies are presented in separate pages, except IC 3418 which we did not detect in HI and thus is not included in the atlas. In Figure 4 we show the outline of each page. The contour levels of the HI emission in the channel maps, the HI surface density in the total HI image, the velocities of the velocity field and velocity dispersion images, and 1.4 GHz continuum emission are shown at the left-bottom of each page.

Channel maps

We present the cubes of $\Delta v \approx 10.4 \text{ km s}^{-1}$ for all galaxies, except NGC 4606 and NGC 4607, which have channels that are $\Delta v \approx 21 \text{ km s}^{-1}$. The lowest contours represent $\pm 2\sigma$, where σ is the rms per beam per channel. The synthesized beam is shown at the left-bottom corner of the first panel on the top-left, i.e. in the channel with the largest velocity. In the same channel, we indicate the optical size, D_{25} , the optical position angle and inclination with an ellipse. In every channel, the optical center is shown with a cross and, the velocity (in km s^{-1}) is shown in the top-right corner.

HI Distribution and Velocities

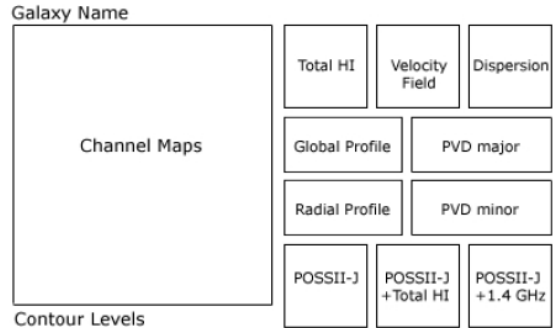


FIG. 4.— This diagram illustrates how the figures are arranged in the atlas, which is appended at the end.

On the top of the right half, the HI surface density distribution (left), the intensity weighted velocity field (middle) and the velocity dispersion (right) are presented with contours overlaid on their own grayscale. The synthesized beam is shown in the bottom-left of the HI surface density image. In the velocity field, the thick-white line represents the HI systemic velocity, V_{HI} measured using the linewidths (§ 5). In the total HI image and the velocity field, the optical major and minor axes (D_{25}) are shown as dotted lines. For 11 systems the optically derived position angle is uncertain because they are either close to face-on with $i \lesssim 45$ or highly warped. For those galaxies we determined the PA kinematically using a tilted-ring model fit on the inner regions of the HI velocity field, where the kinematics is fairly regular. Those galaxies are NGC 4189, NGC 4254, NGC 4299, NGC 4321, NGC 4351, NGC 4394, NGC 4457, VCC 1581, NGC 4689, VCC 2062. The kinematically derived PA's are used throughout the atlas for these galaxies.

Global & Radial profiles

The HI flux density profile and the azimuthally averaged radial HI surface density distribution are shown below the HI surface density distribution. To make the global profiles we measured in each channel the flux density (F_{HI}) in a tight box around the HI area where emission is seen. Throughout the cube we used the areas outside of the HI emission to measure the rms as shown with the error bars. The HI systemic velocity, measured from the HI linewidth (§ 5) is indicated with an upward-pointing arrow.

The azimuthally averaged HI profiles have been derived by fitting tilted ring models, adopting the optically defined center, position angle, and inclination. For galaxies where we derived the position angle based on the HI velocity field, the kinematic PA's were used. The surface density profiles are corrected to face-on and are given in $M_\odot \text{ pc}^{-2}$. The galactocentric radius is given in kpc. The dashed line is the fit using the entire disk, while open circles and solid triangles are fits to the east and the west side separately. For comparison, the optical size of the disk, R_{25} , is indicated with an upper arrow. Of course azimuthally averaged profiles can be misleading, and especially for some of the highly inclined galaxies with known extraplanar gas, such as NGC 4522, NGC 4569, NGC 4330 and NGC 4402, the profiles are of

limited use.

PVDs

On the right side of the global and radial profiles, the position-velocity diagrams (PVDs) along the major axis (upper) and the minor axis (lower) are presented. Again, we adopted the optical center and the position angle for most of the sample to make slices as shown on the upper-right corner of the figures, but we used the kinematically derived PA's for the 11 galaxies mentioned above. The optical center of the cut and the HI systemic velocity as derived from the linewidths (§ 5) are indicated with dashed lines.

Miscellaneous

On the bottom of the right side of each page, we present the POSSII- J (optical B) image (left) and overlays of the HI (middle) and 1.4 GHz continuum contours (right) on the optical image. The optical image itself is shown in high contrast to bring out better the structure of the inner stellar disk, while lower contrast images are used for the overlays to bring out the extent of the stellar disk in comparison to the extent of the HI and the radio continuum emission.

Fully reduced HI data (cubes, moments, XV slices) from the VIVA survey are available in the following URL: <http://www.astro.yale.edu/viva>.

5. HI PROPERTIES

5.1. HI Quantities

In this section, we describe how the HI properties have been determined. The result is presented in Table 3.

Flux (S_{HI}) & Mass (M_{HI})

Column 2 & 3: We have measured the total flux by integrating the global profile along the velocity axis,

$$S_{\text{HI}} = \sum F_{\text{HI}} \cdot \Delta v \pm \left(\sum \sigma_{\text{HI}}^2 \right)^{\frac{1}{2}} \cdot \Delta v \quad (1)$$

in Jy km s^{-1} , where F_{HI} and σ_{HI} are the HI flux and the rms in Jy at each channel, and Δv is the channel width ($\approx 10.4 \text{ km s}^{-1}$). The HI mass in M_{\odot} can be then determined by,

$$M_{\text{HI}} = 2.356 \times 10^5 S_{\text{HI}} D_{\text{Mpc}}^2 \quad (2)$$

in M_{\odot} , where S_{HI} is the total flux in Jy km s^{-1} and D is the distance to the galaxy in Mpc (assumed to be 16 Mpc for all galaxies).

Linewidths (W_{20} , W_{50}) & HI velocity (V_{HI})

Column 4, 5 & 6: The linewidths have been measured at 20% and 50% level of the peak fluxes on both the receding and the approaching sides of the profile,

$$W_{20} = V_{20}^R - V_{20}^A \quad (3)$$

$$W_{50} = V_{50}^R - V_{50}^A$$

where V_{20}^R , V_{50}^R and V_{20}^A , V_{50}^A are the velocities with 20%, 50% of the peak flux on the receding and the approaching sides, respectively. The HI velocity has been determined with V_{20}^R , V_{50}^R and V_{20}^A , V_{50}^A using the following definition,

$$V_{\text{HI}} = 0.25 (V_{20}^A + V_{50}^A + V_{50}^R + V_{20}^R). \quad (4)$$

The uncertainties in W_{20} , W_{50} and V_{HI} are approximately 10.4 km s^{-1} .

Diameters ($D_{\text{HI}}^{\text{iso}}$ & $D_{\text{HI}}^{\text{eff}}$)

Column 7 & 8: To determine the isophotal diameter we use the radius where the azimuthally averaged HI surface density (Σ_{HI}) drops to $1 M_{\odot} \text{ pc}^{-2}$. If there is more than one radius with $\Sigma_{\text{HI}}=1 M_{\odot} \text{ pc}^{-2}$ (e.g. in case an HI hole is present in the central area on the disk), we take the outermost position to derive the isophotal diameter. NGC 4293 is the only galaxy where $D_{\text{HI}}^{\text{iso}}$ is not defined in this way since Σ_{HI} is always below $1 M_{\odot} \text{ pc}^{-2}$. For this galaxy we use as effective diameter the region that contains 50% of the total flux. We also determined isophotal and the effective diameters for the east and the west sides of the disk, separately. The difference between these and the diameters measured over the entire disk, i.e. $\Delta E = D_{\text{east}} - \bar{D}$ and $\Delta W = D_{\text{west}} - \bar{D}$, is a useful measure of the morphological asymmetry.

Deficiency (def_{HI})

Column 9: The HI deficiency is an indicator of how HI deficient individual galaxies are compared to field galaxies of the same size and morphological type. Haynes & Giovanelli (1984) have defined def_{HI} as follows,

$$def_{\text{HI}} = \langle \log \bar{\Sigma}_{\text{HI}}(T) \rangle - \log \bar{\Sigma}_{\text{HI}}, \quad (5)$$

where $\bar{\Sigma}_{\text{HI}} \equiv S_{\text{HI}}/D_{\text{opt}}^2$, is the mean HI surface density within the optical disk. This mean surface density varies only slightly with Hubble type, T , for types Sab-Sm, but varies more for types Sa and earlier. For isolated galaxies, Haynes & Giovanelli (1984) empirically determined $\langle \log \bar{\Sigma}_{\text{HI}}(T) \rangle = 0.24, 0.38, 0.40, 0.34$, and 0.42 for Sa/Sab, Sb, Sbc, Sc, and later types than Sc respectively. However, Koopmann & Kenney (1998) have shown that Hubble classification does not work for many cluster spiral galaxies in Virgo, due to environmental processes which remove gas and greatly reduce star formation rates. We therefore prefer to use the type independent HI deficiency parameter, which compares all morphological types to a mean HI surface density ($\langle \log \bar{\Sigma}_{\text{HI}} \rangle = 0.37$; Haynes & Giovanelli 1984). We use as the uncertainty in the deficiency the difference between the type independent deficiency and the type dependent deficiency using the morphological types from the RC3 catalog (Table 1), $\Delta_{def_{\text{HI}}} = |def_{\text{HI}}(T) - def_{\text{HI}}|$.

HI mass-to-light ratio (M_{HI}/L) in B & K

Column 10 & 11: The HI mass to light ratio in B and K -band in solar unit (M_{\odot}/L_{\odot}) has been measured using the following equations,

$$\begin{aligned} \frac{M_{\text{HI}}}{L_B} &= 1.51 \times 10^{-7} S_{\text{HI}} 10^{0.4(m_B - A_B)} \frac{M_{\odot}}{L_{\odot, B}}, \\ \frac{M_{\text{HI}}}{L_K} &= 1.15 \times 10^{-6} S_{\text{HI}} 10^{0.4(m_K - A_K)} \frac{M_{\odot}}{L_{\odot, K}} \end{aligned} \quad (6)$$

where S_{HI} is in Jy km s^{-1} , and A_B and A_K are the Galactic extinction in B and K -band, taken from the Lyon-Meudon Extragalactic Database (LEDA; Paturel et al. 1997) and NED (NASA/IPAC Extragalactic Database). In Table 3, the values are given in logarithmic scale. The K -band magnitude (Kron magnitude measured at 20 mag arcsec $^{-2}$) has been obtained from the 2MASS

(The Two Micron All Sky Survey; Skrutskie et al. 2006) database.

HI-to-optical size ($D_{\text{HI}}^{\text{iso}}/D_{\text{opt}}$) in B & K

Column 12 & 13: The ratio of the HI isophotal diameter to the B and K -band optical diameters are presented. The B band diameters (listed in Table 1) are D_{25} from RC3. The K -band diameters have been obtained from the 2MASS database (Kron isophotal diameters at 20 mag arcsec $^{-2}$). No photometric measurements are available for several systems that are faint in K .

5.2. Comparison of total HI flux with values in the literature

In this subsection we compare the VIVA fluxes (VLA C or CS array) with either the fluxes measured in the Arecibo Legacy Fast ALFA (ALFALFA) survey of the Virgo region (Kent et al. 2008) or for the few galaxies that have not yet been observed with ALFALFA with the most reliable fluxes listed in ARECIBO-05. We also compare our flux values with the earlier imaging surveys by Cayatte et al. (1990; VLA D array) and Warmels (1988a and b; WSRT imaging and one-dimensional strip scans, respectively). The latter surveys have much lower signal to noise than the VIVA data, but have different UV coverage. Arecibo has a filled aperture and is less likely to miss flux. However, its beam is quite large ($\sim 3.5'$ at 21 cm) and the total flux within one beam can be confused by other systems. It can also miss some flux in case a galaxy with HI extent larger than the beam is observed with a single pointing. However the new seven element Arecibo L-band Feed Array (ALFA) receiver system makes a complete image of the area and we consider the ALFALFA fluxes the best measure of the total amount of HI. Meanwhile interferometers cannot measure structures on angular scales larger than the fringe spacing formed by the shortest spacing (Taylor et al. 2004). As a result they can miss some flux in extended features. The VLA CS array has the same shortest spacing as the VLA D array, and it should in principle be able to measure extended features equally well (the maximum extended structure that can be imaged is 15 arcmin at 20 cm). However since it has fewer short spacings than D array it still somewhat less sensitive to faint extended structure. With the VLA C array, the maximum extent visible is 6 arcmin and we could possibly have missed some flux from very extended structures in the galaxies observed with the C configuration. Our conclusion is that in general there is very good agreement with the ALFALFA fluxes.

In the upper plot in Figure 5 we show a comparison of the ALFALFA fluxes with the VIVA fluxes (filled symbols). Open symbols are single dish measurements taken from ARECIBO-05. There is good agreement between the interferometer and the single dish values. Since there is a distinct possibility that the interferometer resolves out some of the most extended flux, we show in the lower plot the difference between the single dish values and the VIVA flux as function of HI extent. As expected the scatter in the total flux goes up in absolute value for large sources, but the fractional error goes down. There is no evidence that VIVA fluxes are less than ALFALFA fluxes for the large diameter sources. Rather, there is a marginally significant suggestion that VIVA fluxes are

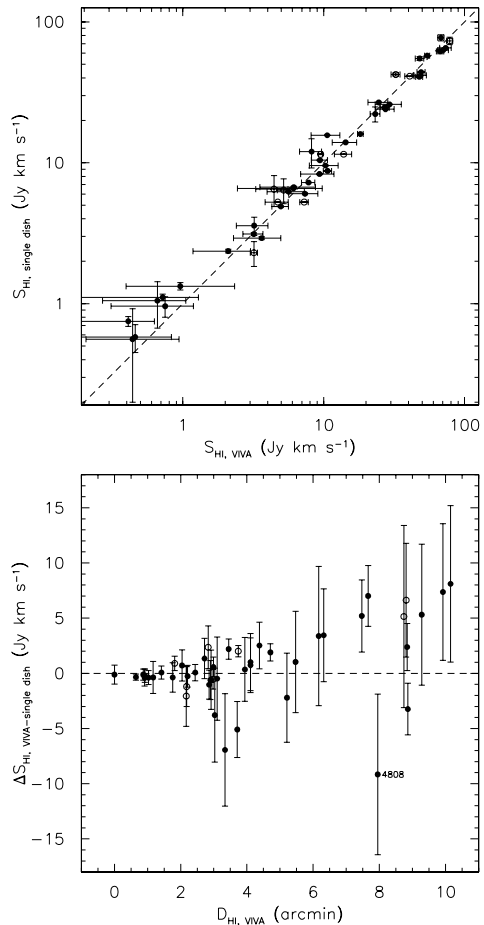


FIG. 5.— Top) A comparison of the single dish fluxes and the VIVA fluxes. The ALFALFA and the ARECIBO-05 fluxes are shown in filled and open circles, respectively. Bottom) The difference between the VIVA and the single dish flux as function of HI extent.

on average greater than ALFALFA fluxes for the largest sources. To estimate how significant the uncertainties in the flux values are we show in Figure 6 (upper plot) the same differences, but normalized by the VIVA fluxes. Clearly there is good agreement for the large size sources. Interestingly there appears to be a very small systematic bias for the smaller size sources. The VIVA fluxes are all below the single dish value although this is a small effect compared to the size of the error bars. We believe this to be the result of the way we make the total HI images, by using a cutoff in the smoothed images.

Finally, mostly for historical interest, we show in the bottom plot of Figure 6 the difference between the VIVA flux and the values measured by Cayatte et al. (1990) and/or Warmels (1988a, b), normalized by the VIVA flux as function of HI diameter. There is excellent agreement, except for NGC 4535. Interestingly both Cayatte et al. (1990) and Warmels (1988b) find a 20% larger flux for this galaxy, on the other hand there is excellent agreement between the ALFALFA and VIVA flux. We have no explanation for this discrepancy.

In conclusion we find that there is excellent agreement between the VIVA and ALFALFA fluxes and there is no indication that the interferometer has missed any very extended flux.

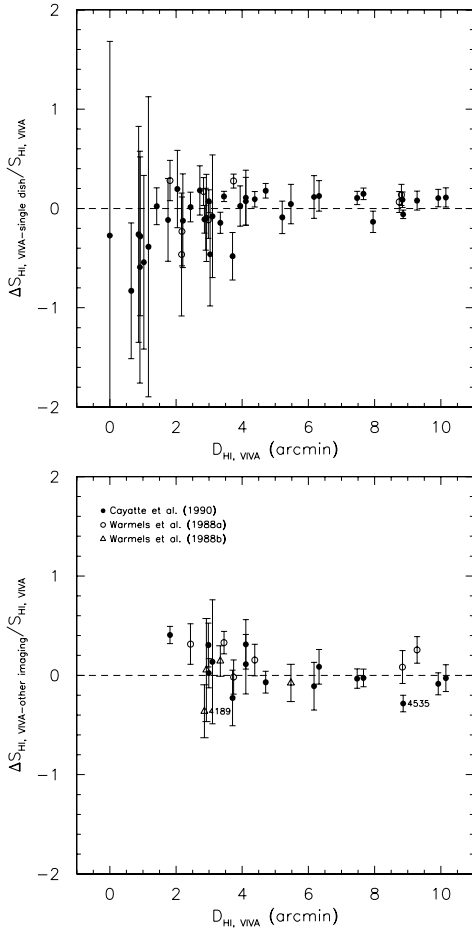


FIG. 6.— Top) The difference between the VIVA and the single dish flux normalized by the VIVA flux as function of HI extent. The same symbols are used as Figure 5. Bottom) Same as above but a comparison with the previous VLA imaging study (Cayatte et al. 1990; filled circle) or WSRT (Warmels 1988a; open circle) imaging study and 1-dimensional observations (Warmels 1988b; open triangle).

6. THE HI MORPHOLOGY IN DIFFERENT ENVIRONMENTS

In this section we describe the range of HI morphologies found in the different locations in Virgo. We present results for individual galaxies in an appendix. In Figure 7 we show a composite image of the total HI images of the individual galaxies (in blue) overlaid on the ROSAT X-ray image (orange) by Böhringer et al. (1994). The galaxies are located at the proper position in the cluster but each HI image is magnified by a factor 10 to show the details of the HI distribution. The picture shows how non-uniform the mass distribution in Virgo is, with enhanced X-ray emission from the cluster and subclusters centered at the giant ellipticals, M87, M86 and M49 respectively. There is a huge range in HI size of the galaxies. In general the galaxies at larger projected distances have larger HI sizes, while galaxies in the core have small HI sizes, but there are exceptions. In Figure 8 we show typical examples for the range of morphologies that we see.

HI rich galaxies in the outskirts of the cluster

HI rich galaxies are exclusively found in the lower density regions of the cluster outskirts at the projected distance

from M87 $d_{87} \gtrsim 1$ Mpc. These galaxies usually have HI extending well beyond the stellar disk in all directions. Small, kinematically distinct HI features with or without optical counterparts are quite common around these systems. A typical example is NGC 4808 shown in Figure 8. Many of the galaxies in the outskirts look morphologically peculiar showing tails or rings in HI, in the stellar distribution or both. Some show a kinematical decoupling between inner and outer gaseous disks. These galaxies seem to be experiencing gravitational interactions and possibly continuing infall of gas from the halo. For example NGC 4651 (Figure 8) shows in HI an extension to the west, while deep optical images show a stellar tail to the opposite side of the HI, which ends with a low surface brightness arc. Kinematically the HI disk shows a discontinuity in position angle between inner and outer disk.

Long one-sided HI tails pointing away from M87

At intermediate distances from M87 ($0.6 \lesssim d_{\text{M87}} \lesssim 1$ Mpc), we find seven galaxies with long one-sided HI tails pointing away from M87. An example is NGC 4302 (Figure 8). The HI is mildly truncated within the stellar disk in the south, and the gas tail is extended to the north, with no optical counterpart. Although there is a nearby companion, NGC 4298, NGC 4302 looks optically undisturbed. In Chung et al. (2007) we argue that these galaxies have only recently arrived in the cluster and are falling in to the center, likely on highly radial orbits as hinted by the direction of the tails. A simple estimate suggests that all but two of the tails could have been formed by ram pressure stripping of the gas in the very outer parts of the disk. Some of these galaxies have close neighbours, suggesting that tidal interactions may have moved gas outward, making it more susceptible to ram pressure stripping. Apparently galaxies begin to lose their gas already at intermediate distances from the cluster center through ram pressure stripping and tidal interactions or a combination of both.

Symmetric HI disks with $D_{\text{HI}}/D_{\text{opt}} \approx 1$ at intermediate distances At similar distances from M87 as the HI tails we find galaxies with fairly symmetric HI disks that are comparable in size to their stellar disk, e.g. NGC 4216 shown in Figure 8. Some are quite HI deficient, despite the fact that the HI extent is comparable to the optical extent. Their HI surface density is down by up to a factor two. These systems might be under the influence of a process that slowly affects the entire face of the galaxy, such as turbulent viscous stripping or thermal evaporation (Nulsen 1982; Cayatte et al. 1994).

Small HI disks near the cluster center Near the cluster core ($d_{\text{M87}} < 0.5$ Mpc) galaxies always have gas disks that are truncated to within the optical disk. These galaxies often show highly asymmetric HI distributions as they are currently undergoing strong ram pressure stripping. An example is NGC 4402 (Figure 8), which has been studied in detail by Crowl et al. (2005). Galaxies appear to lose most of their HI gas ($> 70\%$) in these regions through a strong interaction with the ICM.

Severely stripped HI disks beyond the cluster core Interestingly, we also find a number of galaxies that are stripped to well within the stellar disk at large projected distances from the cluster center ($\gtrsim 1$ Mpc). Examples are NGC 4522, NGC 4405, and NGC 4064 (Figure 8). Some of these may have been stripped while

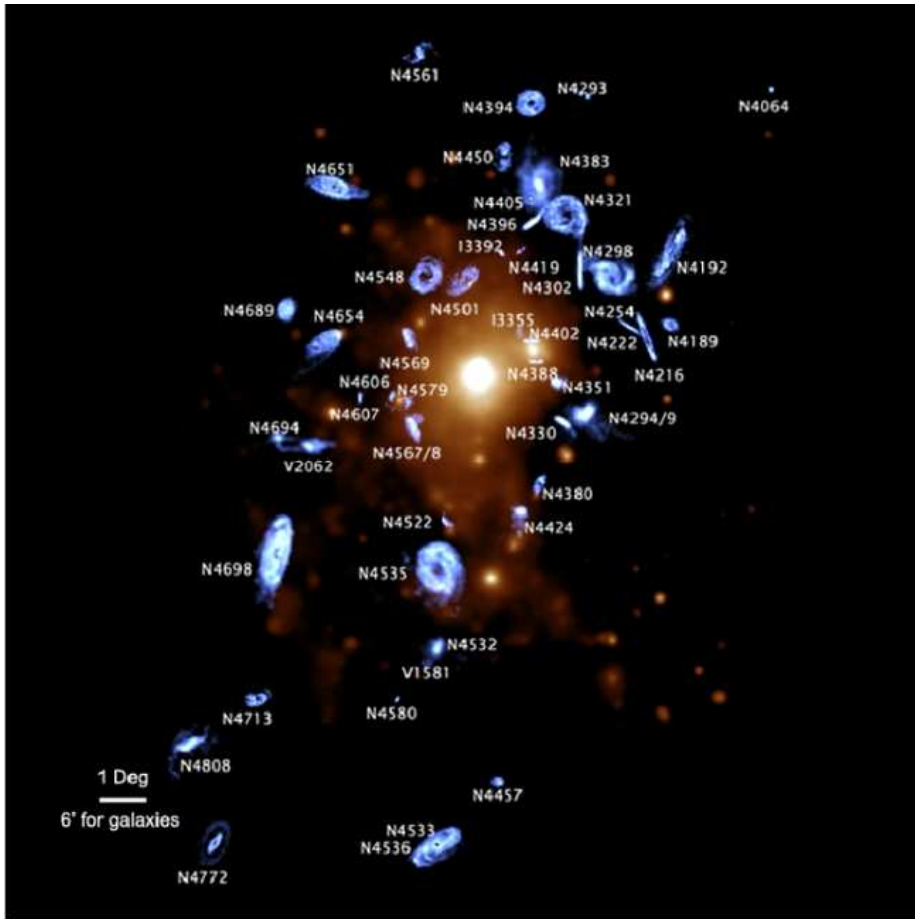


FIG. 7.— A composite image of the total HI images of the individual galaxies (in blue) overlaid on the ROSAT X-ray image (orange) by Böhringer et al. (1994). The galaxies are located at the proper position in the cluster but each HI image is magnified by a factor 10 to show the details of the HI distribution. The picture shows clearly how non uniform the mass distribution in Virgo is, with enhanced X-ray emission from the three subclusters centered at the ellipticals, M87, M86 and M49.

crossing the cluster center. As the galaxies move out from the high ICM density region stripped and disturbed gas that is still bound to the galaxy may resettle onto the disk and form a small symmetric gas disk in the center (NGC 4405). However, a detailed study of the mean stellar age at the truncation radius by Crowl & Kenney (2008) shows that some of these galaxies have been forming stars until recently (< 0.5 Gyr). This leaves not enough time for these galaxies to have been stripped in the center and then travelled to their current location. NGC 4064 is a good example of this. It must have lost its gas at large distances from the cluster center.

A particularly interesting case is NGC 4522 (Kenney et al. 2004), which shows abundant evidence for current ongoing strong ram pressure stripping despite its large projected distance from M87 (≈ 1 Mpc). An estimate of the mean stellar age at the stripping radius (Crowl & Kenney 2006) also suggests that stripping is ongoing, yet an estimate of the ram pressure at that location based on a smooth distribution of the ICM would indicate that pressure is too low by a factor 10. Kenney et al. (2004) argue that merging of the sub cluster M49 with Virgo could locally enhance the ram pressure, due to bulk motions, clumpy density distributions and variations in the temperature of the ICM gas. A temperature map of the X-ray emission

(Shibata et al. 2001) does show that NGC 4522 is located near strong variations in the X-ray temperature. The results on galaxies such as NGC 4064 and NGC 4522 fit in nicely with recent work by Tonnesen, Bryan & van Gorkom (2007) and Tonnesen & Bryan (2008), who find that ram pressure can vary by more than a factor 10 at a given distance from the cluster center due to structure in the ICM. This makes it possible for some galaxies to get stripped in the outskirts, without ever making it to the center of the cluster, something we may be witnessing in Virgo.

7. SUMMARY

We present the results of a new HI imaging survey of 53 galaxies in the Virgo cluster. The goal is to study the impact of different environmental effects on the HI disks of the galaxies. Virgo is ideal for this type of study as it is dynamically young and potentially contains galaxies that are affected by a wide range of environmental effects. Its nearness allows us to study individual galaxies in great detail.

We have selected 48 galaxies and obtained data on 5 additional galaxies that were in the same field and velocity range as the target galaxies. The galaxies were selected to cover a wide range of star formation properties from anemic to starburst, and to be located in a

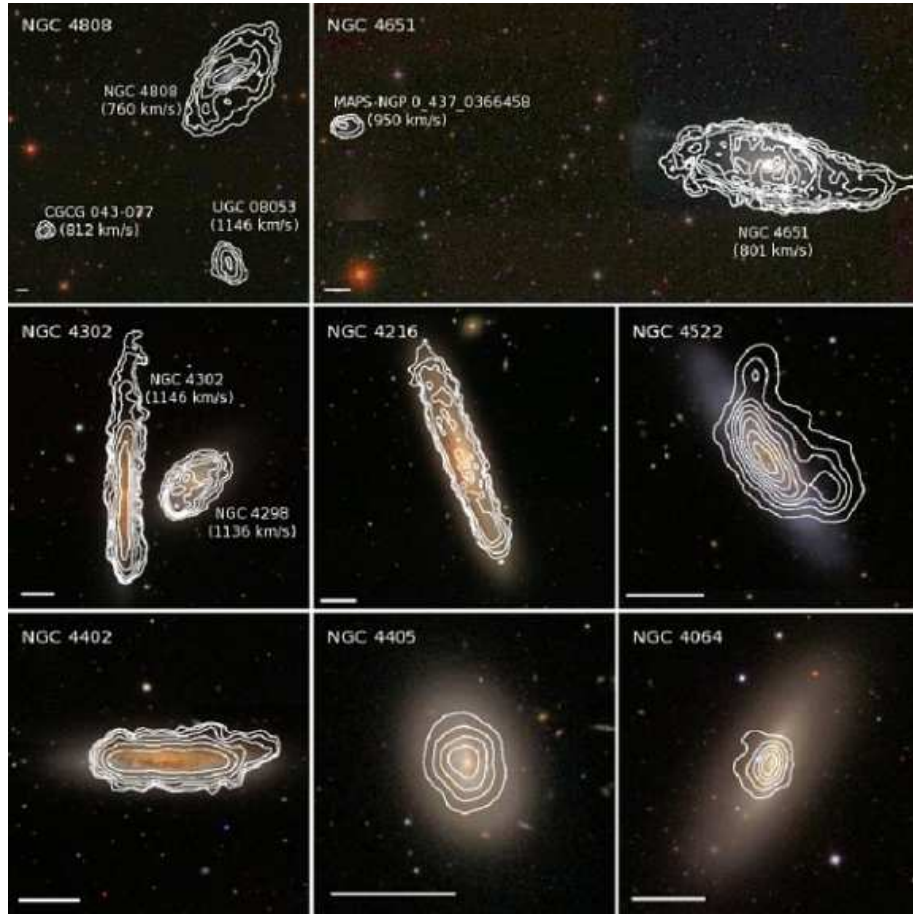


FIG. 8.— Examples of the different HI morphologies found in the survey. Total HI images are shown in white contours overlaid on the Sloan Digital Sky Survey (SDSS) images. The thick white bar in the bottom left corner indicates 1 arcmin in each panel. The top row shows examples of gas rich galaxies in gas rich environments in the outskirts, the middle row shows galaxies at intermediate distances, while the bottom row shows examples of severely truncated HI disks at a range of projected distances from M87.

wide range of local galaxy densities, from the dense core to the outskirts of the cluster. The target galaxies are at projected distances from 0.3 to 3.3 Mpc from the cluster center and as such the survey covers a region that is 2 to 3 times larger than the area explored in the previous VLA survey by Cayatte et al. (1990). Many of our galaxies had never been imaged in HI. The new survey was done with the VLA CS configuration. Its spatial and spectral resolution are a factor 3 and 4 better than that of the previous survey. The VIVA survey has not only confirmed results from previous HI imaging studies, it has found many features that were never seen before in Virgo, or any other cluster. To summarize our main results:

1. We confirm that galaxies near the cluster center have HI disks that are much smaller than the optical disk. We see however extraplanar gas near some of the galaxies, providing the first direct evidence for ongoing ram pressure stripping and fall back of stripped gas.
2. At intermediate distances from the center (0.6-1 Mpc) we find galaxies with long one-sided HI tails pointing away from M87. Chung et al. (2007) argue that these are most likely galaxies falling into the cluster on highly radial orbits. The tails are

due to ram pressure stripping and in a few cases to the combined effect of gravitational interactions and ram pressure stripping. Thus the impact of ram pressure begins to affect galaxies already at intermediate distances from the center.

3. We found several galaxies in the outskirts of Virgo ($d_{87} > 1.5$ Mpc) that have also HI disks that are much smaller than the stellar disks. Some of these were already known to be strongly HI deficient (Sanchis et al. 2002). Although these galaxies are as HI deficient as the galaxies in the core, none of them shows signs of ongoing/recent stripping. Some of these galaxies may have been stripped earlier when passing through the center of Virgo, but at least some of them have been forming stars in the stripped part of the disks until quite recently (Crowl & Kenney 2008). The latter galaxies almost certainly have been stripped of their gas in the outskirts of the cluster.
4. In the outskirts we find several extended HI bridges and optical disturbances, which indicate that the systems are gravitationally interacting.

In Paper II we will do a statistical analysis of our HI imaging results and discuss the importance of various

environmental effects on the evolution of cluster galaxies.

The VIVA collaboration has been growing over time. We are grateful for many useful discussions with our colleagues who have joined more recently, David Schiminovich, Eric Murphy, Tomer Tal, Anne Abramson, Ivy Wong, Tom Oosterloo. We thank the ALFALFA consortium for making their data so promptly available to the scientific community. We thank the anonymous referee for comparing the VIVA data to single dish data from GOLDMINE and providing us with plots of the excellent agreement. This work has been supported by NSF grants 00-98294 and 06-07643 to Columbia University and by grant 00-71251 to Yale University. This work has been supported by NASA grant 1321094. This research has made use of the NASA/IPAC Extragalactic Database (NED) which is operated by the Jet Propulsion Laboratory, California Institute of Technology, under contract

with the National Aeronautics and Space Administration. The Digitized Sky Survey was produced at the Space Telescope Science Institute under US government grant NAG W-2166. This publication makes use of data products from the Two Micron All Sky Survey, which is a joint project of the University of Massachusetts and the Infrared Processing and Analysis Center/California Institute of Technology, funded by the National Aeronautics and Space Administration and the National Science Foundation. Funding for the SDSS and SDSS-II has been provided by the Alfred P. Sloan Foundation, the Participating Institutions, the National Science Foundation, the U.S. Department of Energy, the National Aeronautics and Space Administration, the Japanese Monbukagakusho, the Max Planck Society, and the Higher Education Funding Council for England. The SDSS Web Site is <http://www.sdss.org/>.

APPENDIX

COMMENTS ON INDIVIDUAL GALAXIES

In this section, we describe the HI morphology and kinematics of individual galaxies in detail and compare them with data at other wavelengths. Unless otherwise mentioned, the optical R -band and $H\alpha$ morphology and surface brightness profiles are from Koopmann et al. (2001) and Koopmann & Kenney (2004a, b). For the radio continuum emission we refer to our own 1.4 GHz continuum data, otherwise references are given.

NGC 4064 The HI extends to only about one fifth of the stellar disk (< 4 kpc) and might be slightly extended to the NE. Optically, NGC 4064 has a relatively undisturbed outer stellar disk, with a strong central bar that smoothly connects with open spiral arms in the outer disk. It has strong star formation in the central 1 kpc but virtually no $H\alpha$ emission beyond. Strong radio continuum emission from the central kpc is roughly coincident with the circumnuclear string of luminous HII regions. A detailed morphological and kinematical study of the central regions of NGC 4064 is presented by Córtes, Kenney & Hardy (2006). Along the bar, the stellar, molecular (CO) and ionized ($H\alpha$) gas velocity fields show strong non-circular motions indicative of radial streaming out to a radius of at least 1.5 kpc. The HI velocity field shows no evidence of non-circular motions, but this may be because the bar is not resolved at the resolution of the HI data. It is somewhat of a puzzle why this galaxy has such a severely stripped HI disk. The galaxy is located in the outskirts of the cluster ($d_{87} = 2.5$ Mpc), which makes ongoing ram-pressure stripping due to the ICM seem unlikely. Crowl & Kenney (2008) estimate that star formation in the stripped part of the disk got quenched only 425 Myr ago, while it would take about 2 Gyr for the galaxy to travel from the core to its current location. Thus the gas has not all been stripped in the cluster core. Although some galaxies appear to be stripped by ICM-ISM ram pressure at surprisingly large cluster distances, perhaps due to a dynamic lumpy ICM (Kenney et al. 2004; Crowl & Kenney 2008), NGC 4064 does not seem fully consistent with this scenario. While the outer stellar disk looks undisturbed, the large radial gas motions and circumnuclear starburst suggest a recent gravitational interaction. NGC 4064 may have experienced the combined effects of a gravitational interaction and gas stripping in the cluster outskirts (Tonnesen et al. 2007) although the details remain uncertain.

NGC 4189 The HI disk is slightly more extended than the optical disk. The velocity field and position velocity slices show that the disk has a symmetric warp. Enhanced HI emission is found to the south east, where a clumpy $H\alpha$ ridge is present. The radio continuum shows enhanced emission along that same ridge in the south east. Its Tully Fisher distance estimate puts it significantly further than the Virgo mean distance (Gavazzi et al. 1999; Solanes et al. 2002), and Binggeli et al. (1985) argue that it belongs to the M cloud. HI emission has been also detected from two dwarf galaxies at similar velocities within < 50 kpc distances (Fig. A9). This makes it even more likely that NGC 4189 is in the background. If close to the cluster, the dwarfs would have been stripped of their HI.

NGC 4192 The HI is more extended to the south east which is clearly seen in the PVD and the flux density profile. The velocity field shows distortion in the center which might be due to the presence of a bar (Warmels 1988a; Bosma 1981). The outer HI disk shows a warp. Warmels (1988a) reported an extended disk emission in continuum at 1.4 GHz, which we also have detected in spite of a small number of line-free channels. It has been classified as normal in $H\alpha$. See also Cayatte et al. (1990).

NGC 4216 It is fairly regular in the HI distribution but has a depression in the center as shown by the radial surface profile. Its HI extent is slightly less than the optical extent. The overall HI surface density, however, is low for a spiral galaxy of this size. It is its HI surface density, that makes this galaxy HI deficient. The velocity field looks regular but shows non-circular motions in the outer parts (see the velocity field). No radio continuum has been detected. A prominent dust lane is present. Perhaps this galaxy has been affected by a process that affects the entire surface of the disk, such as viscous turbulent stripping or thermal evaporation.

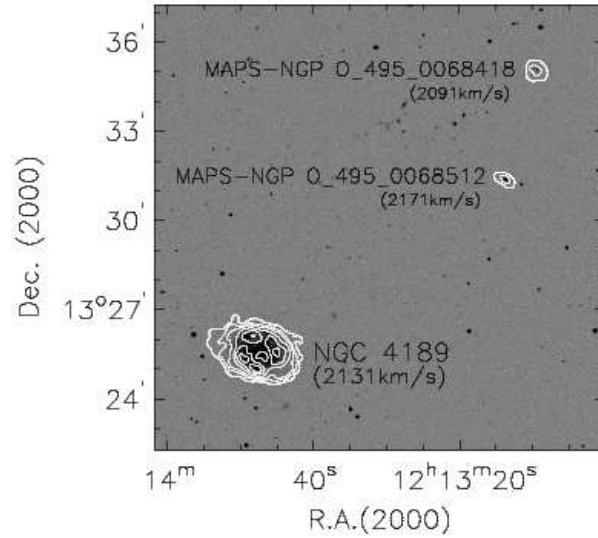


FIG. A9.— The HI distributions of NGC 4189 and two dwarf neighbors are shown in white contours overlaid on the Digital Sky Survey (DSS) image.

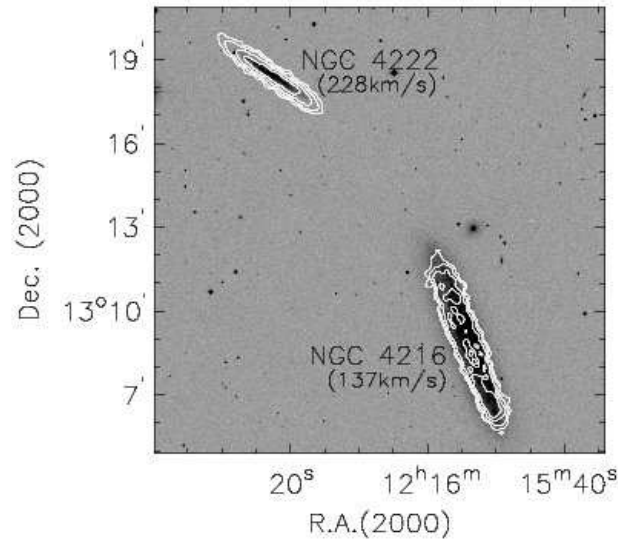


FIG. A10.— The HI distributions of NGC 4216 and NGC 4222 are overlaid on the DSS image. Both galaxies appear to be warped in the outer HI disk.

NGC 4222 The HI extent is larger than the optical extent. The gaseous disk appears to be warped in the southwest as is apparent from the HI velocity field and the PVD. This galaxy was found in the same field as NGC 4216 ($d \approx 56$ kpc in projection, $\Delta v = 280 \text{ km s}^{-1}$, see Figure A10). We do not find any clear signatures of interactions between the two, although it is interesting to see mild distortions at the edge of the disk in both systems. Unlike NGC 4216, NGC 4222 is not HI deficient and does not have an unusually low HI surface density, yet there is one more similarity, it is also not detected in radio continuum.

NGC 4254 As a prototypical one armed spiral galaxy, NGC 4254 has been the subject of many studies. The HI morphology is highly asymmetric with a low surface brightness extension to the north. Optically, the one outstanding spiral arm winds around from the south to the southwest. The HI follows this stellar arm. However just south of this arm, faint HI emission can be seen in the total HI image. These are the peaks of a giant HI tail imaged with Arecibo by Haynes, Giovanelli and Kent (2007). The tail wraps around NGC 4254 in the west, and then extends north for a total length of 250 kpc. Most of its velocity is around 2000 km s^{-1} , just outside the velocity range probed by the VLA. In that sense it is reminiscent of the long tail found near NGC 4388 (Oosterloo & van Gorkom 2005). The fact that both tails cover a velocity range well outside that of the associated galaxy is perhaps good evidence that these galaxies really are inside the cluster. The tail feels the additional cluster potential. There are however important differences between the tails, NGC 4388 is close to the center of Virgo, and its tail is almost certainly due to ram pressure stripping (Oosterloo & van Gorkom 2005), while NGC 4254 is further from the center of Virgo. Haynes et al. (2007) argue that

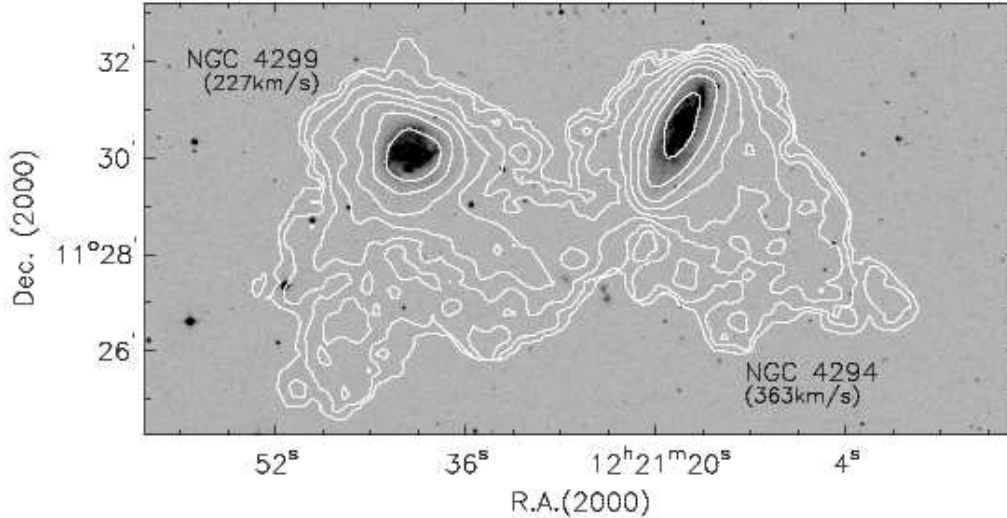


FIG. A11.— The HI distributions (C+D) of NGC 4294 and NGC 4299 are overlaid on the DSS image. Note that both tails are pointing to the same direction to the southwest. The C+D image has revealed a longer tail of NGC 4294 and the second tail of NGC 4299 to the southeast more clearly. This pair of galaxies are located at ~ 0.7 deg distance in projection to the southwest of M87.

the tail of NGC 4254 is probably the result of galaxy harassment, but simulations of Duc & Bournaud (2008) show that the morphology can be reproduced by one rapid close flyby.

NGC 4293 It is one of the two most HI deficient galaxies ($def_{\text{HI}} > 2$) in the sample. The azimuthally averaged HI surface density is everywhere below $1 M_{\odot} \text{pc}^{-2}$ and the HI isophotal diameter ($D_{\text{HI}}^{\text{iso}}$) is not defined. There is no HI emission in the center but its central radio continuum is pretty strong and the emission may be hidden by absorption. This means that in reality we have a lower limit to the total HI mass and an upper limit to the HI deficiency. In fact weak redshifted HI absorption is seen in the center which indicates the presence of non-circular motion. It is truncated/anemic in $\text{H}\alpha$ morphology. The misalignment between the outer stellar envelope and the inner stellar disk suggests a gravitational disturbance (Cortés 2005). This may be responsible for both the truncation in HI and non-circular motion in the center.

NGC 4294 (*Tango I*) Within the stellar disk, the HI morphology and kinematics are quite regular. The HI is slightly more extended to the southeast but the asymmetry is not significant along the major axis. Along the minor axis however, a long HI tail is found on one side to the southwest, which had been completely missed by Warmels (1988a). The length of the tail is about 23 kpc. The full data set, including both C and D-array data, show that the length of the tail is about 27 kpc. The HI tail does not have a stellar counterpart down to a limiting magnitude of $r = 26 \text{ mag arcsec}^{-2}$ in the Sloan Digitized Sky Survey. The stellar disk looks more diffuse in the southeast while a strong spiral arm can be seen the northwest side of the disk. The star formation property has been classified as normal (Koopmann & Kenney 2004b). However the $\text{H}\alpha$ morphology is quite asymmetric in the same way as the radio continuum with more emission to the northwest (Koopmann et al. 2001). The lack of a stellar counterpart makes it less likely that a tidal interaction is the only cause of the tail. However, NGC 4299 is only 27 kpc away, and the two galaxies have almost the same velocity, with $\Delta v \approx 120 \text{ km s}^{-1}$. A gravitational interaction between the two galaxies cannot be ruled out (Fig. A11). See also the comments on NGC 4299 and Chung et al. (2007).

NGC 4298 The HI is more extended and diffuse to the northwest while the other side of the disk shows a sharp cutoff (see Fig. A12). The HI rotation curve is also slightly asymmetric, rising more steeply in the north west. The radio continuum emission shows a central point source and extended emission to the south east, coinciding with the compressed HI. The stellar disk on the other hand is more extended to the north west at the opposite side of the HI compression. NGC 4302 is only 11 kpc away in projection with $\Delta v \approx 30 \text{ km s}^{-1}$. The two galaxies are likely to be a physical pair, and an interaction might well have caused the lopsidedness of NGC 4298. A tidal interaction is less likely to be solely responsible for the HI morphology of NGC 4302. See also Chung et al. (2007).

NGC 4299 (*Tango II*) HI compression is seen to the southwest and a long HI tail is found to the southwest. This tail is pointing to the same direction as NGC 4294’s HI tail without a stellar counterpart down to the SDSS limit. The fact that the tails are parallel makes it less likely that it is only a tidal interaction which has caused the tail. However, NGC 4299 shows some hints for tidal interactions as well. Optically it has a very small/weak bulge and weak spiral arms which are highly asymmetric. Also as shown in Figure A11, a much broader tail HI is found to the southeast, which looks similar to tidal debris (Mihos 2003). As we argue in Chung et al. (2007), the pair, NGC 4294 and 99 are likely to be under the influences of both ICM pressure and as tidal interaction. The $\text{H}\alpha$ emission is enhanced to the south.

NGC 4302 The HI is mildly truncated within the optical disk to the south while a long tail is present to the opposite side (Fig. A12, see also Chung et al. 2007). Its HI PVD presented here and in Chung et al. (2007) shows a “figure-

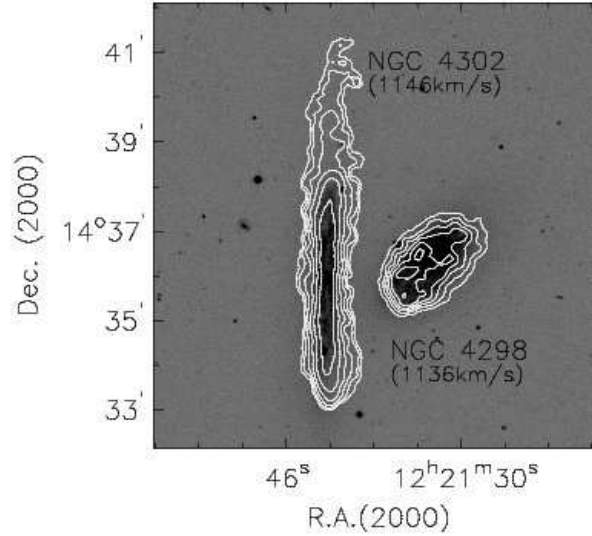


FIG. A12.— The HI distributions of NGC 4298 and NGC 4302 are overlaid on the DSS image. They are only 11 kpc and $\approx 30 \text{ km s}^{-1}$ away from each other. This pair of galaxies are located at 0.9 deg distance to the northwest of M87 with velocities close to the cluster mean motion.

of-eight” feature. NGC 4302 appears to be box-shaped in the optical. These features suggest an edge-on view of a thickened bar (Bureau & Freeman 1999). The radio continuum is found along the prominent dust lane. The mild truncation of the HI to within the optical disk to the south suggests that this galaxy is undergoing ram pressure stripping, possibly also the cause of the HI tail seen to the north (Chung et al. 2007).

NGC 4321 This galaxy has an HI disk which is slightly larger than the optical disk. It has a low surface brightness extension to the south west, coinciding with a very faint optical arm. The velocity field shows that the disk is slightly warped in the south west. An HI depression is present in the center. NGC 4321 has a nuclear stellar bar and a prominent ring of circumnuclear star forming regions (Wyder et al. 1998). The radio continuum emission peaks in the center possibly contributing to the central depression in HI. A faint optical bridge is present to the northeast which is connected to a dwarf companion, NGC 4323, at only 24 kpc distance away in projection, with a velocity difference of $\Delta v \approx 300 \text{ km s}^{-1}$.

NGC 4330 The HI is much more extended to the southern side of the disk than the northern side. The northeast side of the HI disk ends with a sharp cutoff. On the other side an extended HI tail is seen, starting well within the optical disk, but curving south-southwest. Along the western edge of the tail, radio continuum emission is seen. There is no optical counterpart down to the SDSS surface brightness limit (Chung et al. 2007), but the western side of the HI tail is also detected by GALEX (Fig. 2), indicative of recent star formation. Chung et al. (2007) have argued that the galaxy is undergoing ram-pressure stripping as it enters the cluster for the first time. More extensive discussion based on multi-wavelength data on this particular galaxy will appear in Abramson et al. (2009, in prep).

NGC 4351 (Stubby tail) The HI shows a short and broad extension in the southwest and a sharp cutoff to the northeast. It has a modest HI deficiency, and the HI and optical extents are similar. Its PVD is also asymmetric, showing a flat velocity gradient to the northeast but a decreasing velocity gradient to the southwest. The radio continuum is quite strong to the northeast, the same side where the HI compression is found. Its location ($d_{87} \lesssim 0.5 \text{ Mpc}$) and extreme velocity w.r.t. Virgo ($\Delta v > 1000 \text{ km s}^{-1}$) suggest that the galaxy may be radially falling into the cluster, and possibly experiencing strong ICM ram pressure. However, the nucleus and the optically brightest parts of the inner galaxy are significantly offset from the centroid of the outer galaxy isophotes, and the outer stellar disk shows suggestions of shell-like structure. Thus some of the galaxy’s peculiarities are likely caused by a gravitational disturbance.

NGC 4380 The HI distribution shows a mild asymmetry in a sense that the northwest disk is overall more dense compared to the southeast disk which shows a slightly low HI surface density but extended. In the middle, little HI is found and the radio continuum is very weak. Optically, the galaxy has a very weak bulge with a low surface brightness stellar disk without clear spiral features. Its $H\alpha$ morphology has been classified as truncated/anemic. There is a hint of a stellar ring to the northwest where the highest HI column density is found. The galaxy is somewhat HI deficient without any obvious signatures of ongoing or recent ICM-ISM interaction.

NGC 4383 (Crazy) This is one of the most HI rich galaxies in the sample with $def_{\text{HI}} \lesssim -0.8$. The HI extent is enormous compared to the optical disk ($D_{\text{HI}}^{\text{iso}}/D_{25} > 4$). Within the stellar disk, its HI kinematics and morphology seem fairly regular, although even within the central $2'$ the major axis PVD shows some low velocity gas and the minor axis PVD shows some non-circular motions. Beyond this radius, the HI distribution and kinematics are irregular. There is a clear kinematical distinction between the inner (within the optical disk) and the outer HI, with different kinematic major axes suggestive of an irregular warp. Along the entire eastern side there is a sharp kinematical discontinuity $\sim 2\text{-}3'$ from the nucleus, whereas in the west the transition is more gradual. The outer HI shows weak $m=2$ spiral

structure, with a weak arm to the south-southeast, and a somewhat stronger one to the north-northwest. The outer HI in the east-northeast forms a single irregular arm unrelated to the $m=2$ pattern. Along the same eastern side as this irregular arm, but beyond the main body of HI there are two distinct gas clouds: one to the east just beyond the main body of HI, but with a velocity which is $\sim 20 \text{ km s}^{-1}$ offset, and the other $7'$ to the southeast. It is not impossible that both clouds are high surface brightness peaks in a more extended very low surface brightness structure. $\text{H}\alpha$ and UV emission are observed from roughly the same area as the stellar disk, with very little from the region of extended HI, except for a UV counterpart to the inner HI spiral arm in the north. NGC 4383 is a starburst galaxy, with strong $\text{H}\alpha$ and UV emission from the central $\sim 1'$, and a biconical $\text{H}\alpha$ nebula along the minor axis suggestive of an outflow. The galaxy is likely influenced by a combination of gas accretion and tidal interaction. The small galaxy 2.5 arcmin to the southwest of NGC 4383 is UGC 07504 (VCC 0794), a Virgo cluster galaxy with a velocity of 918 km s^{-1} . This velocity is offset by 800 km s^{-1} from NGC 4383, thus they are not gravitationally bound, and probably not physically associated. The velocity range of UGC 07504 is entirely outside the range of our VLA HI observations, however the galaxy is undetected in radio continuum, $\text{H}\alpha$, and single dish HI observations (ARECIBO-05).

NGC 4388 Our VLA data show that the HI is very deficient, truncated and asymmetric within the stellar disk, with a much greater extent to the east. There is an HI "upturn" extending vertically upwards (north) from the outer edge of the HI disk in the west, suggestive of ongoing ram pressure from the southwest. WSRT observations show a $\sim 100 \text{ kpc}$ long plume of HI extending toward the northwest of NGC 4388 (Oosterloo & van Gorkom 2005). The HI mass in this plume is similar to the HI mass remaining in NGC 4388. The plume is smoothly connected with NGC 4388 both spatially and in velocity and has no optical counterpart, suggesting that the HI plume is gas that was ram pressure stripped from NGC 4388 within the last few hundred Myrs. This plume was missed in the VIVA survey due to the limited bandwidth and reduced sensitivity at large distances from the field center. The highest HI surface densities of the plume gas occur beyond the halfwidth of the primary beam of the VLA and at that point the velocities of the gas are outside the velocity window of our observations. We note that the VIVA integrated profile is very asymmetric with an excess of HI at the high velocity side, where the plume connects with the disk. Yoshida et al. (2002) and Kenney et al. (2008) find very extended extraplanar $\text{H}\alpha$ emission which might have originated from stripped cool ISM shocked by the hot ICM and/or the central AGN. This ionized gas is almost certainly part of the HI tail. Both the major and minor axis PVD's show redshifted absorption, indicative of non-circular motions. NGC 4388 was the first Seyfert galaxy discovered in Virgo (Phillips & Malin 1982), and its nuclear activity has been detected at many wavelengths (e.g. Veilleux et al. 1999; Yoshida et al. 2002; Iwasawa et al. 2003). It was also one of the first spiral galaxies in which anomalous radio continuum was detected with an elongated component crossing the nucleus and perpendicular to the optical disk (Hummel et al. 1983). Here we detect strong radio continuum emission from the AGN, as well as emission from the star-forming disk with almost the same extent and asymmetry as the HI disk.

NGC 4394 (*Fruit Loop or Life Saver*) The HI is quite deficient and is mildly truncated within the stellar disk. The HI morphology and kinematics are remarkably regular and symmetric. An HI hole is found in the middle which is quite common for strongly barred galaxies like NGC 4394. Optically the galaxy is slightly asymmetric in the sense that the northeast spiral arm is more prominent than the one in the southwest. Its $\text{H}\alpha$ classification is anemic, and its radio continuum emission is correspondingly very weak. It has a large apparent neighbor, the S0 galaxy NGC 4382 (M85) at $\approx 35 \text{ kpc}$ projected distance with a velocity difference of $\Delta v \approx 200 \text{ km s}^{-1}$. Although NGC 4382 has stellar shells suggesting that it might be a merger remnant (Schweizer & Seitzer 1992) we find neither in HI nor at other wavelengths any signatures of a tidal interaction between the two galaxies.

NGC 4396 (*Crocodile*) This galaxy has a prominent HI tail to the northwest (Chung et al. 2007) but unlike other Virgo galaxies with HI tails clearly caused by ram pressure, the origin of NGC 4396's tail is unclear. HI contours are compressed to the south, but not at the southeast end of the major axis, as would be expected if this were the leading edge of a strong ICM-ISM interaction (as is seen in NGC 4330, NGC 4388, NGC 4402). $\text{H}\alpha$ and broadband images show that the distribution of star formation is asymmetric with only one prominent spiral arm found to the southeast. Radio continuum emission is strong in the center, and within the disk it is stronger in the southeast where the one prominent $\text{H}\alpha$ spiral arm is located. There is no radio continuum or UV emission associated with the HI tail, contrary to what is seen in NGC 4330, NGC 4402, and NGC 4522. Deep optical imaging reveals that the outer NW stellar disk is gas-free and the HI tail leaves the stellar disk, consistent with a ram pressure stripping origin. However, there is no "radio deficit" observed at the SE outer edge (Murphy et al. 2009), as expected for strong active ram pressure, thus the origin of the features in NGC 4396 are not completely clear.

NGC 4405 The HI is highly deficient and strongly truncated, and the stellar disk appears normal. The $\text{H}\alpha$ image shows relatively normal star formation in the central 30% of the stellar disk and is sharply truncated beyond that. There are no compressed HI contours or significantly disturbed kinematics, so there is no evidence for ongoing ICM pressure. Its radio continuum is quite strong and slightly asymmetric with a possible extension to the southwest. Its properties are consistent with a strong ram pressure stripping event at least a few hundreds Myr ago (Crowl & Kenney 2008).

NGC 4402 The HI is moderately deficient, moderately truncated within the undisturbed stellar disk, and asymmetric. Within the disk, the HI extends further west than east. The HI contours are compressed in the SE and a modest HI tail exists to the NW, suggesting active ram pressure from the SE. The radio continuum has an extended tail to the NW, extending further from the disk than the HI. The position angle of this tail matches those of elongated dust filaments which Crowl et al. (2005) have interpreted as dense clouds being ablated by ram pressure. Further evidence of strong ram pressure acting from the SE comes from the enhanced radio continuum polarization (Vollmer et al. 2007) and the radio continuum deficit region in this area (Murphy et al. 2009). As shown in Figure A13, several neighbors have

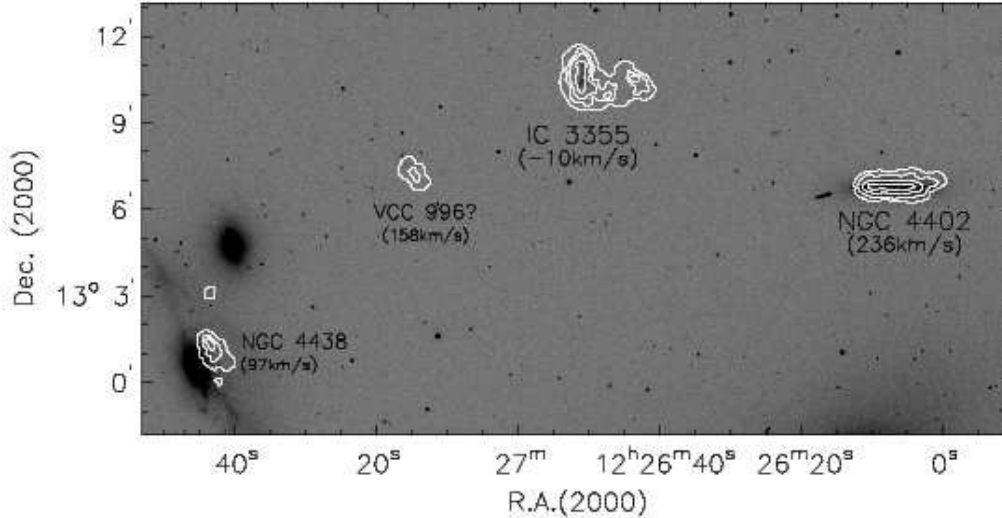


FIG. A13.— The HI distributions of NGC 4402 and its neighbors are overlaid on the DSS image. The projected distance between NGC 4402 and NGC 4438 is ≈ 122 kpc at the Virgo distance. Mihos et al. (2005) have presented a deeper optical image of this region.

been detected in the same field: IC 3355, which is in the VIVA sample, and NGC 4438, which is known for its optical peculiarities with a small HI disk. We also found a small HI cloud somewhere between IC 3355 and NGC 4438 at the velocity of ≈ 160 km s $^{-1}$. It seems very possible that VCC 996 ($v = -28$ km s $^{-1}$), whose optical center is only only 55'' from the HI peak of the cloud, is its optical counterpart.

IC 3355 (*Casper*) This is a peculiar low-mass, HI-rich object whose origin is unclear. Optical images show an elongated stellar body with no clear nucleus, a high surface brightness ridge with a sharp cutoff in the east, and lower surface brightness emission extending to the west. HI emission covers the entire stellar body, with two peaks that straddle the galaxy center. There are no compressed contours and no clear evidence of active ram pressure. The HI velocity field shows a very modest gradient across the main body, and the overall pattern is not one dominated by rotation. A small HI cloud with no known optical counterpart is present 2' to the west, connected by an HI bridge which extends from the southern part of the stellar body. The small HI cloud exhibits a larger velocity gradient (~ 50 km s $^{-1}$) than the main body of the galaxy, but there is no clear rotation pattern. The line-of-sight velocity of IC 3355 is near zero, and its membership to Virgo is controversial (Hoffman et al. 1988; Cayatte et al. 1990). However, it is unlikely to be in the Local Group, since the stellar light distribution is too smooth for such a nearby system. If it is in the Virgo cluster, its velocity and proximity on the sky to M86 make it very likely that this galaxy is associated with the M86 group. This galaxy is located 11.5' (~ 55 kpc projected) from the spiral NGC 4402, $\sim 16.9'$ (~ 79 kpc projected) from M86, and $\sim 16.8'$ (~ 78 kpc projected) from the disturbed spiral NGC 4438. However, its Virgo membership might be questioned because 1) more massive galaxies in this neighborhood are severely stripped in HI (e.g. NGC 4438; Cayatte et al. 1990 and NGC 4402; Crowl et al. 2005), while this galaxy is HI rich and 2) in a recent deep optical image of this region (Mihos et al. 2005), this galaxy appears to be located outside of a huge common envelope of intracluster light (ICL) around the M86 group. Nonetheless, it is possible that IC 3355 is a member of the M86 group and has not yet been gas stripped. Its HI properties suggest it may have been disturbed by a gravitational interaction.

NGC 4419 The HI is highly deficient and severely stripped within the stellar disk ($D_{\text{HI}}^{\text{iso}}/D_{25} < 0.5$). It has very strong radio continuum emission from a nuclear source, likely an AGN (Decarli et al. 2007), plus weaker extended emission co-spatial with the H α emission that traces the anemic star formation in the disk. Some HI is observed in absorption against the bright nuclear source, as shown in the PVD diagrams. This absorbing gas is redshifted by ~ 100 km s $^{-1}$ with respect to the nucleus, providing evidence for non-circular motions in the central region. The presence of absorption has reduced the amount of HI seen in emission, and accounts for the relative paucity of HI emission observed near the nucleus. Thus the plots of the integrated HI emission and the radial distribution underestimate the amount of HI present near the nucleus. This is the only galaxy for which the otherwise excellent agreement with linewidths measured by ALFALFA breaks down, the width measured with VIVA is almost 200 km s $^{-1}$ larger. However the profile shapes are in very good agreement and we suspect that ALFALFA must have been misled by the absorption and not included the component at -100 km s $^{-1}$. Optical images show an undisturbed stellar disk. There is neither extraplanar HI emission detected in this highly inclined spiral, nor compressed HI contours, so there is no direct evidence of ongoing ram pressure. There may however be some hints of rather recent stripping. The outer HI extent is somewhat asymmetric with more emission in the SE part of the disk, and optical images show disturbed dust lanes. CO emission is also strongly asymmetric in the disk of NGC 4419, but in the opposite sense from the HI, since there is more CO to the NW than to the SE (Kenney et al. 1990). The stellar population study of Crowl & Kenney (2008) shows that star formation in the gas-free outer disk stopped ~ 500 Myr ago, and the galaxy could be experiencing fall-back after peak ram pressure.

NGC 4424 (*Jellyfish*) This is a very peculiar HI-deficient galaxy. It is one of the galaxies with long one-sided HI tails pointing away from M87 (Chung et al. 2007). The stellar disk is strongly disturbed, with shells and banana-shaped isophotes. There is strong star formation in a bar-like string of HII complexes in the central 1 kpc, and no star formation beyond (Kenney et al. 1996). The radio continuum is quite strong in the circumnuclear region, and shows two distinct off-nuclear peaks coincident with the brightest star forming complexes. The central region also contains disturbed dust lanes and disturbed ionized gas kinematics (Cortés et al. 2006). This all clearly indicates a strong gravitational interaction, either a merger or close collision. Chung et al. (2007) find that the HI extent is much smaller than the optical disk along the major axis while it has a remarkably long HI tail to the south (≈ 18 kpc at least). One end of the tail is curved to the southeast, pointing almost directly to M49, the giant elliptical at the center of the M49 sub-cluster, which is ≈ 0.44 Mpc away. In a recent follow-up study with the WSRT (Oosterloo, van Gorkom & Chung, in preparation) the HI tail appears to extend over > 40 kpc. Interestingly, the HI cloud that Sancisi et al. (1987) found near M49 is at the same velocity as NGC 4424's HI tail. This suggests a collision between NGC 4424 and M49 as a possible explanation for the peculiarities of NGC 4424. Further study is required to distinguish between this and other scenarios.

NGC 4450 The HI is overall moderately truncated with low surface density. Less HI is detected along the minor axis but this could be because the low surface density gas is just below our detection threshold on the minor axis, where gas is spread out more in velocity. An HI depression is present in the center where there is a weak stellar bar. Strong radio continuum is detected from the nucleus, probably from an AGN. Optically the galaxy shows tightly wound but weak spiral structure and anemic star formation. No obvious evidence for tidal or ongoing ICM-ISM interactions are found.

IC 3392 The HI is severely truncated within the undisturbed stellar disk with $D_{\text{HI}}^{\text{iso}}/D_{25} < 0.5$. In the channel maps there is a hint of an HI extension along the minor axis, to the northwest. The HI distribution is fairly symmetric, there are no compressed HI contours, and the HI velocity field is regular, thus we do not find any signatures of ongoing pressure. The stellar population study of Crowl & Kenney (2008) shows that star formation in the gas-free outer disk stopped ~ 500 Myr ago, thus the galaxy seems to have been gas-stripped a while ago and is no longer in an active phase of stripping. It is located only ≈ 125 kpc away in projection from NGC 4419 but the systemic velocities differ by ($\Delta v \sim 1900$ km s $^{-1}$), and the galaxies are unlikely to be physically related.

NGC 4457 The HI extent is smaller than the optical disk and quite asymmetric with the HI peak offset from the optical center toward the southwest. This HI peak coincides with the galaxy's one strong and peculiar spiral arm, which is very prominent in H α . Quite strong radio continuum is present with almost the same extent as the HI. There are no compressed HI contours, and therefore there is no evidence for active ICM pressure. The velocity field suggests that the HI disk is slightly warped, but there are no obvious signature of a tidal interaction in the HI kinematics or optically.

IC 3418 (*Ghost*) This is a peculiar low surface brightness system (IBm) found $\sim 1^\circ$ to the southwest of M87, with a tail of UV emission to the SE. We have not detected HI in this galaxy over the velocity range we searched (-250 to 250 km s $^{-1}$). Until very recently, the galaxy's velocity and even its Virgo membership was not well-known, and HI could exist outside our search window. Within our velocity window, the HI upper limit is $\sim 8 \times 10^6 M_\odot$ assuming a linewidth of 100 km s $^{-1}$. The first velocity measured using optical spectroscopy was 25662 ± 74 km s $^{-1}$ but with low reliability (Drinkwater et al. 1996). The observed very extended UV morphology (Fig. 2) makes it extremely unlikely that the galaxy is that distant. More recently Gavazzi et al. (2004) published an optical spectroscopic velocity of 38 km s $^{-1}$ which we adopted for the HI observations. This redshift was recently confirmed (Crowl, private communication) in a spectrum taken with LRIS at Keck. The velocity measured is $\approx 0 \text{ km s}^{-1} \pm 50 \text{ km s}^{-1}$. Despite our non detection it is still possible, that the galaxy has a very faint and extended HI disk. If it were smoothly distributed over an area of 3×1 arcmin 2 as it is in UV, the noise goes up roughly by $\sqrt{3 \times 13.9} (\approx 6.5)$ with CS array (i.e. proportional to square root of number of independent beams), which could have been missed in the VIVA study. We note that it has also not been detected in ARECIBO-05 and with ALFALFA, which covers the entire velocity range of the Virgo cluster. It is quite possible that its HI has been completely stripped if the galaxy is a true member of Virgo and close to M87 (its projected distance to M87 is only 0.28 Mpc). In that case the UV stream may have originated from recent star formation due to the compression of the stripped HI gas.

NGC 4501 This large Sc galaxy is mildly HI-deficient. To the SW the HI disk is mildly truncated within the stellar disk and has compressed contours, whereas to the NE the HI is more extended and diffuse. These features have long been known from previous data (Warmels 1988a; Cayatte et al. 1990), and are suggestive of an ongoing ICM-ISM interaction (Cayatte et al. 1990). Our new data with better resolution and sensitivity show additional key details, such as the HI arm in the outer NE region with disturbed kinematics. Detailed comparisons with simulations suggest that NGC 4501 is in an early stage of ram pressure stripping (Vollmer et al. 2008). The compressed HI contours in the SE are coincident with a ridge of strongly enhanced radio polarization (Vollmer et al. 2007) indicating the SE as the leading edge of the ICM-ISM interaction. This is the side closest to M87, which suggests that NGC 4501 is currently entering the high density region of the cluster for the first time.

NGC 4522 (*Cashew*) The highly inclined Sc galaxy NGC 4522 is one of the clearest cases of ongoing ram pressure stripping. This galaxy was observed by Kenney et al. (2004) as a pilot study of the VIVA survey. Its HI has been stripped to well within the optical disk (to $0.35R_{25}$ along the major axis) but there is significant extraplanar HI on one side of the disk. The peaks in the extraplanar HI are located just above the gas truncation radius in the disk, a gas morphology indicative of ram pressure stripping. The old stellar disk (R-band image) is relatively undisturbed, implying that ram pressure and not tidal interactions are responsible for the disturbed gas distribution. The extra-

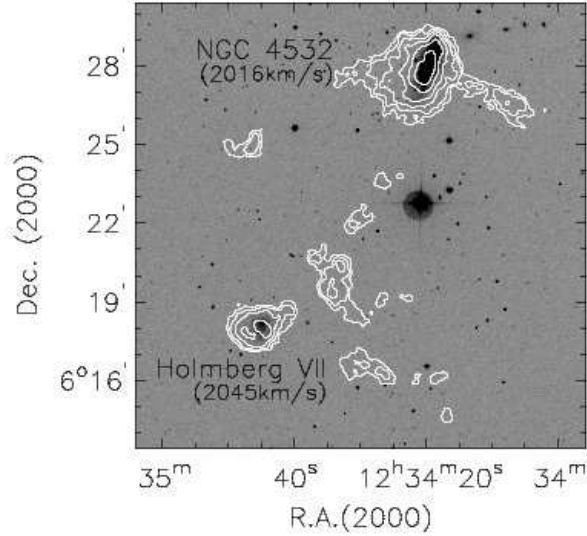


FIG. A14.— The HI distributions of the NGC 4532 region is shown overlaid on the DSS image. Only the C array data of Hoffman et al. (1999) is shown while the total flux is well consistent with theirs combined with the D array data. More sensitive HI data taken with the Arecibo data (ALFALFA survey; Koopmann et al. 2008) have revealed that NGC 4532 and VCC 1581 (Holmberg VII) are embedded in a common HI envelope, which continues to the south as a 500 kpc long HI tail.

planar HI in the west is kinematically distinct from the adjoining disk gas, with velocities offset toward the Virgo cluster mean velocity. Enhanced radio polarization along the eastern edge, on the side opposite the extraplanar HI (Vollmer et al. 2004b), and a deficit of radio continuum emission relative to far-infrared emission beyond the polarized ridge (Murphy et al. 2009) both indicate strong active ram pressure. In a comparison of simulations and data, Vollmer et al. (2006) find that the galaxy is in an active phase of ram pressure stripping, and the best match to the HI morphology and kinematics is 50 Myr after peak pressure. Studies of the stellar population by Crowl & Kenney (2006, 2008) show that star formation in the gas-free outer disk stopped ~ 100 Myr ago, consistent with the stripping time scale from simulations. This galaxy is located at 3.3 deg (~ 0.8 Mpc) from M87, where the estimated ICM pressure, assuming a smooth and static ICM, is too low to remove the HI from the disk. Kenney et al. (2004) have argued that motion or substructure in the ICM, perhaps due to the merging of the M49 group with the main cluster, could have increased the ram pressure on this galaxy. In fact, NGC 4522 is near a local peak in X-ray emission, a ridge where X-ray spectroscopy shows high temperatures possibly indicating a shock front in the ICM (Shibata et al. 2001).

NGC 4532 NGC 4532 is an HI-rich, optically peculiar Sm galaxy with strong H α emission indicating a high star formation rate. In Figure A14 as well as in the atlas, we are presenting the same data as the C-array data of Hoffman et al. (1999). The HI distribution around this galaxy is patchy with several clumps and a remarkably sharp east west extension. Kinematically NGC 4532 appears to be in regular rotation with a warp in the outer parts, the east west feature is kinematically decoupled from the galaxy, and may be the tip of a huge tail seen by ALFALFA (Koopmann et al. 2008). The total flux measured in this region (55.9 ± 1.2 Jy km s $^{-1}$) is consistent with what Hoffman et al. (1999) found in their C+D data (50.9 Jy km s $^{-1}$). The Arecibo Legacy Fast ALFA Survey (ALFALFA) showed recently that NGC 4532 and VCC 1581 (Holmberg VII) are embedded within a large common envelope, which continues to the south as a 500 kpc long HI tail (Koopmann et al. 2008). The extended tail is far outside the primary beam of the VLA and could not have been detected in the VIVA survey. A comparison of the total flux seen by ALFALFA and VIVA shows that there is about as much HI in the diffuse envelope around the pair as there is in the galaxies and small clouds seen by the VLA. It is particularly interesting to compare the velocity fields seen by the VLA and by ALFALFA. The giant tail connects to the galaxy pair in what is called the W cloud (Koopmann et al. 2008) at a velocity of about 1875 km s $^{-1}$, this is the same velocity seen by the VLA west of NGC 4532 in the east-west feature. We conclude then that the huge tail ends in the east west feature seen by the VLA and crosses NGC 4532. NGC 4532 is possibly influenced both by tidal effects and gas accretion.

VCC 1581, Holmberg VII This is an optically faint low-mass galaxy that lies within the huge HI envelope (see Fig. A14) that also covers NGC 4532 (Koopmann et al. 2008). Optically the galaxy has no clear nucleus or symmetry. The HI distribution and kinematics are fairly regular and symmetric, except for a cloud with distinct kinematics 1' NE of the center.

NGC 4535 (Snail) The HI content is relatively normal and HI extends somewhat beyond the stellar disk. Sharp HI cutoffs to the N and NW, towards M87 while further extension to the opposite side of the disk, are suggestive of weak ongoing ram pressure. Vollmer et al. (2007) and Wezgowiec et al. (2007) detect polarized radio continuum in the center and the south west of the outer galactic disk. They argue that this asymmetry is mostly due to an interaction with the ICM. The outermost HI spiral arm to the W and SW is kinematically distinct, with a sharp velocity gradient rather than the more gradual and continuous curvature characteristic of spiral arm streaming motions. There is also

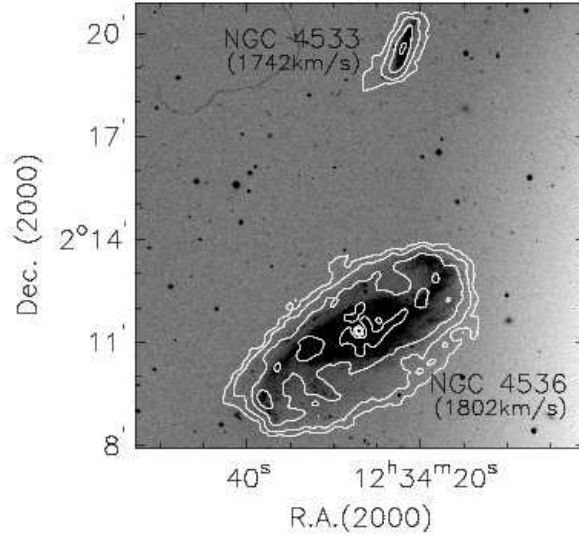


FIG. A15.— The HI distribution of NGC 4536 and NGC 4533 are overlaid on the DSS image. This pair of galaxies, about 39 kpc apart from each other in projection with similar v_{HI} , show some morphological and kinematical peculiarities.

no other spiral arm in the galaxy that shows such kinematic distinctness, supporting the picture that the W/SW arm might be due to ram pressure rather than spiral density waves. It appears similar to the kinematically distinct gas-stripped outer arm of NGC 4569. An HI depression is found in the central 5 kpc where a stellar bar is present. The radio continuum from the nuclear region is quite strong, probably due to an AGN.

NGC 4533 This galaxy has been detected at $\sim 8'$ (39 kpc) distance to the north of NGC 4536 (Fig. A15). The HI is symmetric in the inner parts and has a diffuse asymmetric outer envelope and a short HI tail extends to the south east. Optically it is a small Sd galaxy ($B_T = 14.2$ and $D_{25} = 2.1'$) and its stellar disk also looks asymmetric in the sense that the northwest side is slightly warped and the southeast disk is broader than the north west disk. There are two stellar tails to the southeast, where the HI tail is present. Since this galaxy is close spatially and in velocity to NGC 4536 it is plausible that the two galaxies are gravitationally interacting.

NGC 4536 The HI disk is about the same size as the stellar disk and high column density HI ridges coincide nicely with the optical spiral arms. The galaxy is located in the southern outskirts of the cluster (> 2.8 Mpc from M87) and shows no clear signature of any kind of large disturbance. It is only 39 kpc away in projection from NGC 4533 with $\Delta v_{\text{opt}} < 10 \text{ km s}^{-1}$ (or $\Delta v_{\text{HI}} \approx 50 \text{ km s}^{-1}$). It is possible that this galaxy is responsible for NGC 4533's peculiarities. During the close encounter with NGC 4533, this galaxy may have been less affected because it is more massive (by a factor of $\gtrsim 4$) while NGC 4533 has been quite disturbed. It does however have a small bar in the central $\sim 1'$, apparent in both the optical morphology and the HI PVDs, and the bar might have originated from a tidal interaction.

NGC 4548 The HI is mildly truncated within the optical disk and has a low surface density ($D_{\text{HI}}^{\text{iso}}/D_{25} = 0.86$ and $def_{\text{HI}} = 0.81 \pm 0.01$), resulting in a rather large HI deficiency. An HI hole is found in the central 5 kpc where a strong stellar bar is present. This galaxy was also observed by Vollmer et al. (1999) with a data quality very similar to ours. Vollmer et al. (1999) point out that the faint outer HI arm in the north appears kinematically slightly distinct from the adjacent disk, and suggest that this could have been caused by a past episode of ram pressure. We find no evidence for ongoing ICM pressure or tidal stripping. Kinematically distinct HI is often found in the outer parts of spiral galaxies in the field and it needs not be related to the cluster environment. However, its H α morphology does suggest that NGC 4548 is anemic. The radio continuum emission is extremely weak, even for an anemic spiral (Wezgowiec et al. 2007).

NGC 4561 The HI in this small Sm or Sc galaxy shows the very high surface density in the center while it is very extended, with two open symmetric gas spiral arms reaching far beyond the stellar disk, to 2-3 R_{25} . The gas spiral arms appear to be superposed on a very low surface brightness outer HI disk. There is no evidence of either young or old stars in these HI arms. The HI velocity field shows strong non-circular motions with $m=2$ symmetry, even within the optical disk. There is a small stellar bar in the central $30''$, but this small feature cannot account for the widespread non-circular motions. The HI morphology could either be the result of a merger between two small systems, in which the outer HI is now falling back and forming a new disk (e.g. Barnes 2002), or alternatively it could have been pulled out during an encounter with a nearby galaxy IC 3605 which is ≈ 150 kpc away with $\Delta v = 300 \text{ km s}^{-1}$). The $m=2$ symmetry places strong constraints on any interaction scenario. Lastly the outer HI could be the remains of a giant low surface brightness disk that is now being disturbed by the non axisymmetric stellar body in the center.

NGC 4567 and NGC 4568 This pair of Sc galaxies overlap on the sky (Fig. A16), and their line-of-sight velocities match where the galaxies overlap. Optically neither shows significant disturbances in their inner disks while both look mildly disturbed in their outer parts. Likewise, the HI morphology and kinematics look fairly undisturbed within the brighter parts of the stellar disks. In the outer parts of NGC 4568, HI contours are more compressed in the east, toward

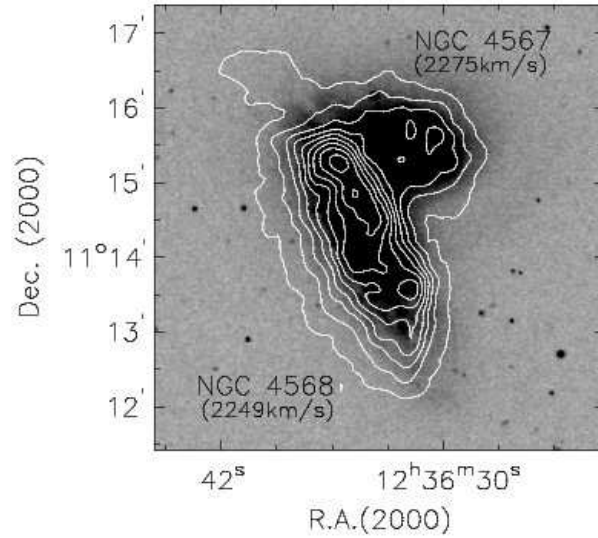


FIG. A16.— The HI distributions of NGC 4567 and NGC 4568 are shown in contours overlaid on the DSS image. The two galaxies do not just overlap due to projection but are actually interacting with each other as the channel maps or the PVDs show clear connections.

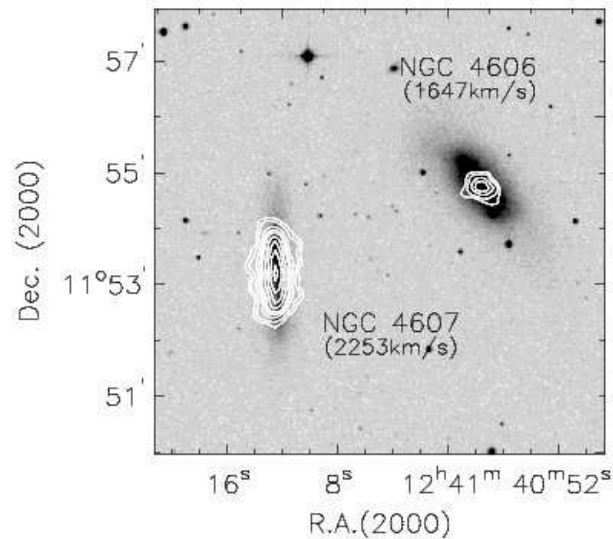


FIG. A17.— The HI distributions of NGC 4606 and NGC 4607 are shown in contours overlaid on the DSS image. The projected distance between the two galaxies is $\lesssim 20$ kpc while $\Delta v \approx 600 \text{ km s}^{-1}$.

NGC 4567, and more extended in the west, where the kinematics suggest a warp or other disturbance. A prominent dust lane at the apparent intersection region between the two galaxies suggests they are physically connected. A little HI tail extends northwest of the pair, and appears to be an extension of the dust lane. The HI morphology suggests that the galaxies are gravitationally interacting, but are in a phase before closest approach so are not yet strongly disturbed. The total HI flux of the pair is consistent with single dish measurements. Since the galaxies overlap both spatially and in velocity, it is difficult (and perhaps not too meaningful) to ascribe an accurate HI flux for each galaxy. The fluxes presented in Table 3 are based on assigning all the flux in the overlap region to NGC 4568, since the HI contours suggest that this may be appropriate.

NGC 4569 The HI disk is only extended about one third of the stellar disk (Kenney et al. in prep). This extraplanar HI, which is kinematically distinct from the disk gas, is very likely gas stripped from the disk by ram pressure. A stellar population study of the gas-free outer stellar disk (Crowl & Kenney 2008) and a comparison of the HI morphology and kinematics with simulations Vollmer et al. (2004a) both indicate that the gas was stripped from the outer disk ~ 300 Myr ago. Radio continuum emission associated with star formation is detected throughout the remaining gas disk (see also Boselli et al. 2006). At fainter levels there is radio continuum emission near the minor axis on both sides extending 24 kpc from the center, likely arising from a nuclear outflow (Chyzy et al. 2006). Due to its negative velocity and large appearance ($\approx 10'$), its cluster membership has been controversial for a long time (e.g. Rodgers & Freeman 1970; Stauffer et al. 1986). Recent

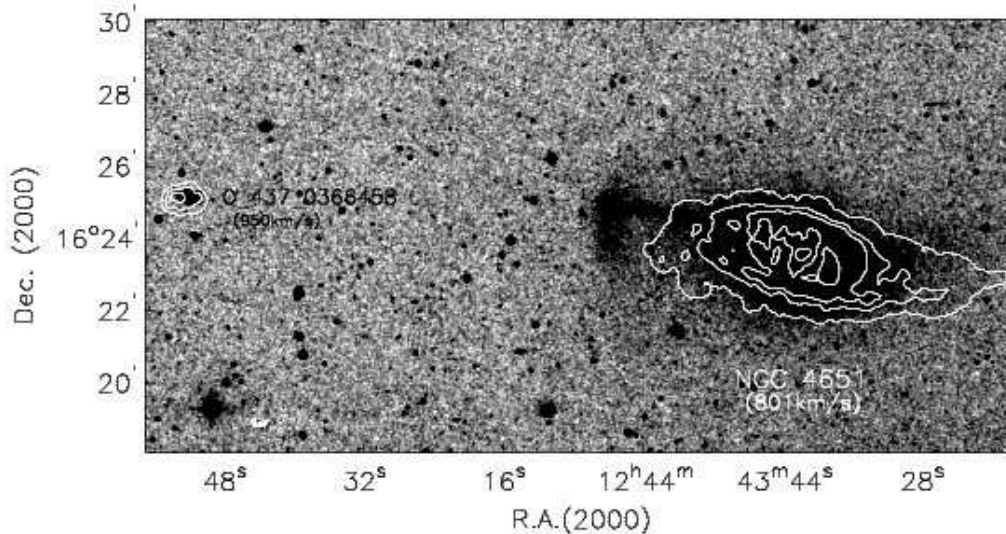


FIG. A18.— The HI contours of NGC 4651 are shown overlaid on a high contrast DSS image. The HI distribution is asymmetric in a sense that it is more extended to the west. In the opposite side of the HI tail, a stellar tail is found, which ends with a shell. On the same side of the disk, we also have detected a small HI cloud of $\approx 2.2 \times 10^7 M_{\odot}$ at ≈ 80 kpc distance from the center of NGC 4651. The cloud has an optical counterpart, MAPS-NGP O_437_0366458 (Canabala 1999).

Tully-Fisher based distance estimates place NGC 4569 somewhat closer than the mean Virgo distance (Solanes et al. 2002; Cortés et al. 2008). The HI evidence for ICM-ISM stripping strongly suggests that NGC 4569 is part of the cluster.

NGC 4579 This galaxy is moderately HI-deficient, and its HI is mildly truncated within the optical disk. But the HI distribution and kinematics appear symmetric and regular, with no indications of any ongoing interaction. There is a deep depression in the central 4 kpc coincident with a stellar bar. The star formation rate is relatively normal in the disk. It has a well-known Seyfert 2 nucleus, with radio jets (Contini 2004). It shows a strong radio continuum emission, both from the nuclear source and the extended star-forming disk.

NGC 4580 The HI is very deficient and severely truncated within the optical disk ($D_{\text{HI}}^{\text{iso}}/D_{25} < 0.5$ and $def_{\text{HI}} > 1$). The $H\alpha$ is also truncated with a sharp edge. The HI peak is slightly offset from the optical center and more emission is present to the southeast. The radio continuum appears more extended than the HI disk in the south. The outer stellar disk appears undisturbed, although it still contains spiral arms. The HI truncation and undisturbed stellar disk strongly suggest an ICM-ISM interaction. The stellar population study of Crowl & Kenney (2008) indicates that star formation stopped in the gas-free outer stellar disk 500 Myr ago. This galaxy is so far from the cluster core that it could not have reached its current location by travelling from the core in only 500 Myr, so it must have been stripped outside the core.

NGC 4606 The HI extends only one tenth of the stellar disk. The HI peak is offset from the optical center with slightly more emission to the west. A faint low surface brightness HI feature extends to the east near the minor axis. The $H\alpha$ is strong in the central kpc but severely truncated within the optical disk and asymmetric in the same way as the HI. The radio continuum is quite strong in the center with almost the same extent as the HI disk. The stellar disk is disturbed (Cortés 2005), with non-elliptical isophotes and a greater extension to the northeast. Disturbed dust lanes are also apparent. This galaxy may have experienced some type of gravitational interaction, although it is not clear what the relative roles of ram pressure and tidal interactions may have been in shaping the HI properties.

NGC 4607 The HI in this edge-on galaxy is truncated to within the stellar disk and the galaxy is strongly deficient in HI ($D_{\text{HI}}^{\text{iso}}/D_{25} \approx 0.7$ and $def_{\text{HI}} = 0.82$). As shown in Figure A17, NGC 4607 is located near NGC 4606 with a projected distance of only about 20 kpc. However, the two galaxies have very different velocities with $\Delta v \approx 600 \text{ km s}^{-1}$ making it unlikely that they are gravitationally bound. Although NGC 4606 looks optically somewhat disturbed, we find no evidence for a tidal disturbance in the optical or HI appearance of NGC 4607.

NGC 4651 While the bright central part of this Sc galaxy (inside R_{25}) appears relatively symmetric and undisturbed both in the optical and in HI, the HI beyond the stellar disk looks more disturbed, possibly warped, and on the western side the HI appears to become more narrow and form a tail-like feature. The HI kinematics of the outer galaxy has a different position angle from the inner galaxy, confirming that the outer HI may be warped. While the inner optical disk is quite symmetric, a high contrast optical image reveals a remarkably straight optical tail to the east which ends at a low surface brightness arc (Figure A18). Although no HI is at the position of the optical tail and arc, Figure A18 shows that 50 kpc away from the stellar shell (and at about 80 kpc distance from the center of NGC 4651) in the direction of the stellar tail there is a small HI cloud of $S_{\text{HI}} = 0.36 \text{ Jy km s}^{-1}$ ($M_{\text{HI}} = 2.2 \times 10^7 M_{\odot}$). The HI cloud has an optical counterpart (MAPS-NGP⁷ O_437_0366458; Canabala 1999). This dwarf galaxy may well have a tidal

⁷ Minnesota Automated Plate Scanner - North Galactic Pole

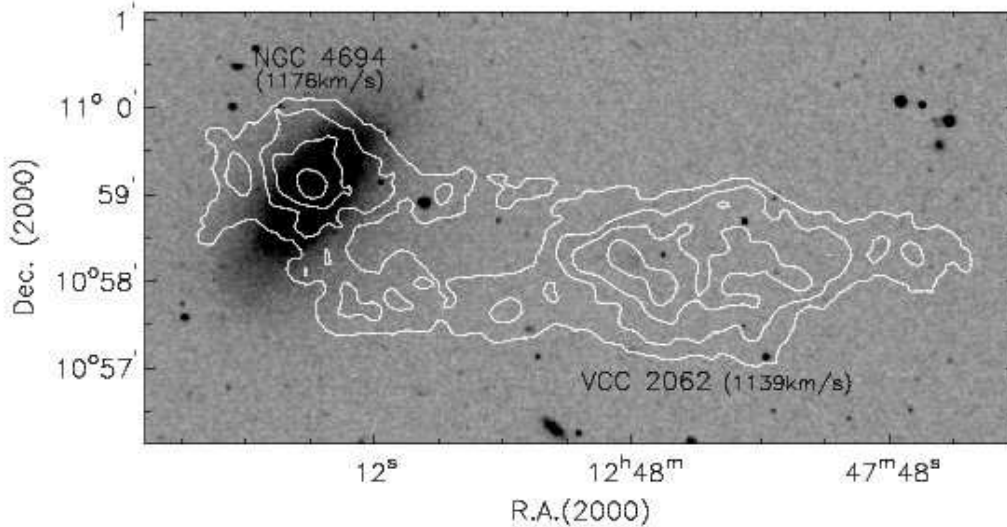


FIG. A19.— The HI distribution of NGC 4694 region is shown overlaid on the DSS image. The HI is stripped on both sides of the stellar disk while short and long extensions are found to the northeast and southwest along the minor axis. The HI feature in the southwest also covers a low surface brightness galaxy, VCC 2062, and extends more than 30 kpc from the center of NGC 4694.

origin. The HI surface density drops steeply in the central 2 kpc. Although there is quite strong radio emission found in the center of the galaxy (50 mJy), the low surface brightness makes it unlikely that the depression in HI is due to absorption.

NGC 4654 We present the same data published in Phookun & Mundy (1995). The HI map shows an extended tail to the southeast and compressed contours to the northwest. Phookun & Mundy (1995) have attributed its HI peculiarities to the ram-pressure due to the ICM. The stellar disk extends beyond the HI in the northwest, suggesting an ICM-ISM interaction. However, the inferred ICM pressure alone may be too low to strip the HI at this location ~ 1 Mpc from M87 (Chung et al. 2007). Alternatively, Vollmer (2003) has shown that the HI morphology and kinematics are best reproduced by a combination of both ram-pressure and a gravitational interaction (e.g., with its neighbor NGC 4639). In fact, the stellar disk also appears to be somewhat disturbed with more diffuse emission to the southeast, which makes it more plausible that a gravitational disturbance took place as well. See also Chung et al. (2007).

NGC 4689 The HI in this galaxy is mildly truncated within the stellar disk with a moderate HI deficiency. The HI morphology and kinematics are fairly regular and symmetric, showing no signatures of ongoing ram pressure or tidal interactions. Weak radio continuum emission is detected over about half the HI disk. The galaxy is also mildly truncated in H α .

NGC 4694 The HI in this galaxy is highly disturbed and irregular, and bears little relation to the stellar disk, as shown in Figure A19. The HI extent along the major axis is much smaller than the stellar disk, but along the minor axis is relatively more extended. The southwest extension is connected to its optically faint neighbor, VCC 2062, and continues well beyond that galaxy. The HI peak within the stellar disk almost coincides with the optical center, however the morphology and kinematics are quite asymmetric along both the major and the minor axes. Overall the HI properties are consistent with an accretion event, and inconsistent with ram pressure stripping. Strong radio continuum emission is present at the center. Optically it has a large bulge with an extended but low surface brightness disk. The lack of HI and star formation in the outer stellar disk, and the disturbed appearance of the central bulge-dominated region, in part due to irregular dust lanes, contribute to its peculiar SB0 or Amorphous classification.

VCC 2062 A huge HI cloud is found to cover both this low surface brightness dwarf galaxy and part of the nearby disturbed spiral NGC 4694 (Fig. A19). The HI peak almost coincides with the position of the highest surface brightness in the optical. Neither the HI nor the optical morphology is well structured while a relatively smooth HI velocity gradient is present across the stellar disk. No radio continuum is found. It is obvious that VCC 2062 is tidally interacting with NGC 4694, although the origin of the stellar component of VCC 2062 is rather unclear, i.e. whether it has tidally formed or it has been destroyed due to the tidal interaction. Recently Duc et al. (2007) have reported their CO detection from this system.

NGC 4698 (*Fish tail*) The HI disk is almost a factor 2 larger than the stellar disk. Its HI morphology and kinematics are fairly undisturbed but two short tails are found to the southeast, while to the northwest, which is toward the cluster center, the HI appears to be fairly compressed. Thus the galaxy may be experiencing weak ram pressure as it approaches the cluster core. Optically it has a low surface brightness ring at the location where $\Sigma_{\text{HI}} \approx 1 M_{\odot} \text{pc}^2$ as well as an inner stellar ring at smaller radii. This galaxy is known for its orthogonally rotating bulge which was optically discovered (Bertola et al. 1999). H α ionized gas kinematics show a clear decoupling of the gas and stellar kinematics in the central few kpc (Cortés 2005), and the HI kinematics show hints of this. The galaxy likely experienced a merger over 1 Gyr ago, and is now experiencing an unrelated episode of early stage ISM-ICM ram pressure stripping.

NGC 4713 (*Crab*) This galaxy has one of the most extended HI disks in the cluster as compared to the optical disk

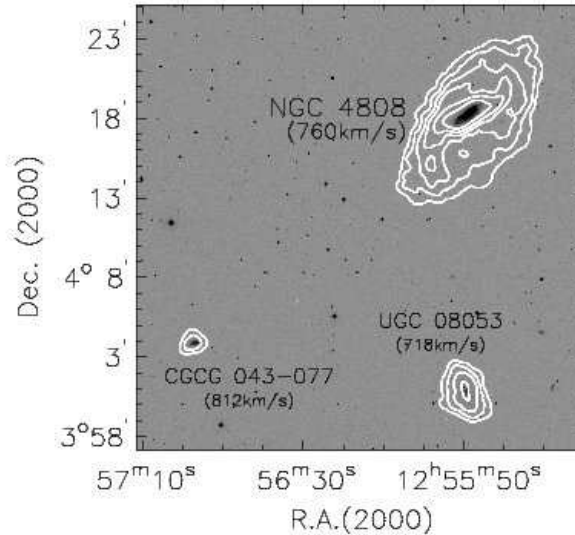


FIG. A20.— The HI distributions of NGC 4808 and nearby dwarfs are overlaid on the DSS image. The combined data of the C and the D configurations are presented. The dwarfs have been discovered in our recent D array follow-up observations.

and shares many properties with NGC 4808, one of its nearest large neighbours in the southern outskirts of the cluster. The HI velocity field suggests a disturbed warp for the gas beyond the stellar disk. There are different HI velocity gradients and position angles on the two sides of the disk. It is classified as an Sc or Sd galaxy, with very strong star formation distributed somewhat irregularly throughout the stellar disk. The HI surface density distribution is has a depression in the center coincident with a stellar bar. A prominent optical spiral arm in the NW lies just inside an outer HI arm. Our HI data for this galaxy are much older and noisier than than most of the VIVA data. Yet our measured total HI flux is only 10% less than the flux measured in the ALFALFA survey, despite our noisy data we recovered almost all of the HI. The radio continuum distribution is also irregular, with an extended off-nuclear peak in the east, and a secondary peak in the west just inside the prominent spiral arm.

NGC 4772 This galaxy was imaged previously by Haynes et al. (2000) in C array. Although our data were taken with CS array and better software was available, including the option to use robust weighting, our results are similar to those of Haynes et al. (2000). A prominent outer HI ring is present. Compared to the inner HI disk, the outer HI ring is at a different position angle and has a lower peak LOS velocity, and may therefore lie in a different plane. The inner HI appears slightly warped at the end of the stellar disk, and the warp feature may connect the inner disk and outer HI ring. Its optical morphology resembles that of NGC 4698 with a strong bulge and a low surface brightness disk. As in NGC 4698 the HI extends well beyond the optical disk. A comparison of stellar and H α gas velocities by Haynes et al. (2000) show central gas components with anomolous velocities. Both the HI properties and the central gas kinematics are suggestive of a minor merger (Haynes et al. 2000), and the relatively symmetric HI and stellar morphologies suggest an older event.

NGC 4808 This galaxy is very HI-rich. The HI is much more extended than the stellar disk, and both the HI morphology and kinematics suggest a strong and asymmetric warp. Optically the galaxy has been classified as Scd with a very weak bulge. There is strong star formation throughout the stellar disk, with an asymmetric and patchy distribution. HI has been detected from two nearby dwarf galaxies in the VLA D array data (Fig. A20). Although no evidence for tidal interactions is found, the three galaxies are located within $\lesssim 60$ kpc distances from each other with similar velocities ($\Delta v < 100 \text{ km s}^{-1}$) and it is very likely that these galaxies are under the influence of one another. Apart from the nearby dwarf galaxies, NGC 4808 shares many properties with NGC 4713, one of its nearest large neighbors in the southern outskirts of the cluster.

REFERENCES

- Aaronson, M., Mould, J., & Huchra, J. 1980, *ApJ*, 237, 655
 Barnes, J. E. 2002, *MNRAS*, 333, 481
 Bekki, K. 1999, *ApJ*, 510, L15
 Bertola, F., Corsini, E. M., Beltrán, V., Pizzella, A., Sarzi, M., Cappellari, M., & Funes, J. G. 1999, *ApJ*, 519, L127
 Bingeli, B., Sandage, A., & Tammann, G. A. 1985, *AJ*, 90, 395
 Boselli, A., Boissier, S., Cortese, L., Gil de Paz, A., Seibert, M., Madore, B. F., Buat, V., & Martin, D. C. 2006, 651, 822
 Bosma, A. 1981, *AJ*, 86, 1825
 Böhringer, H., Briel, U. G., Schwarz, R. A., Voges, W., Hartner, G., & Trümper, J. 1994, *Nature*, 368, 828
 Bravo-Alfaro, H., Cayatte, V., van Gorkom, J. H., & Balkowski, C. 2000, *AJ*, 119, 580
 Briggs, D. S. 1995, PhD Thesis, New Mexico Institute of Mining and Technology, Socorro, NM
 Bureau, M., & Freeman, K. C. 1999, *AJ*, 118, 126
 Cayatte, V., van Gorkom, J. H., Balkowski, C., & Kotanyi, C. 1990, *AJ*, 100, 604
 Cayatte, V., Kotanyi, C., Balkowski, C., & van Gorkom, J. H. 1994, *AJ*, 107, 1003
 Canabala, J. E. 1999, PhD Thesis, University of Minnesota
 Chamaraux, P., Balkowski, C., & Gerard, E. 1980, *A&A*, 83, 38
 Chung, A., van Gorkom, J., Kenney, J. D. P., & Vollmer, B. 2007, *ApJ*, 659, L115
 Chyzy, K.T., Soida, M., Bomans, D.J., Vollmer, B., Balkowski, Ch., Beck, R., & Urbanik, M. 2006, *A&A*, 447, 465

- Contini, M. 2004, MNRAS, 354, 675
- Cortés, J. R. 2005, PhD Thesis, Universidad de Chile
- Cortés, J. R., Kenney, J. D. P., & Hardy, E. 2006, AJ, 131, 747
- Cortés, J. R., Kenney, J. D. P., & Hardy, E. 2008, ApJ, 683, 78
- Cowie, L. L., & Songaila, A. 1977, Nature, 266, 501
- Crowl, H. H., Kenney, J. D. P., van Gorkom, J. H., & Vollmer, B. 2005, AJ, 130, 65
- Crowl, H. H., & Kenney, J. D. P. 2006, ApJ, 649, L75
- Crowl, H. H., & Kenney, J. D. P. 2008, AJ, 136, 1623
- Davies, R. D., & Lewis, B. M. 1973, MNRAS, 165, 231
- Decarli, R., Gavazzi, G., Arosio, I., Cortese, L., Boselli, A., Bonfanti, C., & Colpi, M. 2007, MNRAS, 381, 136
- de Vaucouleurs, G., de Vaucouleurs, A., Corwin, Jr., H. G., Buta, R. J., Paturel, G., Fouque, P., *Third reference catalogue of bright galaxies*, 1991, Springer-Verlag New York, Inc. (RC3)
- Dressler, A. 1980, ApJ, 236, 351
- Drinkwater, M. J., Currie, M. J., Young, C. K., Hardy, E., & Yearsley, J. M. 1996, MNRAS, 279, 595
- Duc, P.-A., Braine, J., Lisenfeld, U., Brinks, E., & Boquien, M. 2007, A&A, 475, 187
- Duc, P.-A., Bournaud, F., ApJ, 673, 787
- Ferrarese, L. and Côté, P., & Jordán, A. 2003, ApJ, 599, 1302
- Gavazzi, G., Boselli, A., Scodreggio, M., Pierini, D., & Belsole, E. 1999, MNRAS, 304, 595
- Gavazzi, G., Zaccardo, A., Sanvito, G., Boselli, A., & Bonfanti, C. 2004, A&A, 417, 499
- Gavazzi, G., Boselli, A., van Driel, W., & O'Neil, K. 2005, A&A, 429, 439 (ARECIBO-05)
- Giovanelli, R., & Haynes, M. 1985, ApJ, 292, 404
- Gómez, P. L., et al. 2003, ApJ, 584, 210
- Gunn, J. E., & Gott, J. R. III 1972, ApJ, 176, 1
- Haynes, M. P., & Giovanelli, R. 1984, AJ, 89, 758
- Haynes, M. P., Jore, K. P., Barrett, E. A., Broeils, A. H., & Murray, B. M. 2000, AJ, 120, 703
- Haynes, M. P., Giovanelli, R., Kent, B. R. 2007 ApJ, 665, 19L
- Hoffman, G. L., Helou, G., & Salpeter, E. E. 1988, ApJ, 324, 75
- Hoffman, G. L., Lu, N. Y., Salpeter, E. E., & Connell, B. M. 1999, AJ, 117, 811
- Hubble, E., & Humason, M. 1931, ApJ, 74, 43
- Hummel, E., van Gorkom, J.H. & Kotanyi, C.G. 1983, ApJ, 682, L85
- Iwasawa, K., Wilson, A. S., Fabian, A. C., & Young, A. J. 2003, MNRAS, 345, 369
- Kenney, J. D. P., Young, J. S., Hasegawa, T. Nakai, N. 1990, 353, 460
- Kenney, J. D. P., Koopmann, R. A., Rubin, V. C., & Young, J. S. 1996, AJ, 111, 152
- Kenney, J. D. P., van Gorkom, J. H., & Vollmer, B. 2004, AJ, 127, 3361
- Kenney, J. D. P., Tal, T., Crowl, H. H., Feldmeier, J., & Jacoby, G. H. 2008, ApJ, 687, 69
- Kent, B. R., Giovanelli, R., Haynes, M. P., Martin, A. M., Saintonge, A., Stierwalt, S., Balonek, T. J., Brosch, N., Koopmann, R. A. 2008, AJ, 136, 713
- Koopmann, R. A., & Kenney, J. D. P. 1998, ApJ, 497L, 75
- Koopmann, R. A., Kenney, J. D. P., & Young, J. S. 2001, ApJS, 135, 125
- Koopmann, R. A., & Kenney, J. D. P. 2004a, ApJ, 613, 851
- Koopmann, R. A., & Kenney, J. D. P. 2004b, ApJ, 613, 866
- Koopmann, R. A., Giovanelli, R., Haynes, M. P., Kent, B. R., Balonek, T. J., Brosch, N., Higdon, J. L., Salzer, J. J., Spector, O. R. A., 2008, ApJ, 682, L85
- Larson, R. B., Tinsley, B. M., & Caldwell, C. N. 1980, ApJ, 237, 692
- Lewis, I., & et al. 2002, MNRAS, 334, 673
- Mei, S., Blakeslee, J. P., Côté, P., Tonry, J. L., West, M. J., Ferrarese, L., Jordán, A., Peng, E. W., Anthony, A., & Merritt, D. 2007, ApJ, 655, 144
- Mihos, J. C. 2004, Clusters of Galaxies: Probes of Cosmological Structure and Galaxy Evolution, p. 277
- Mihos, J. C. 2003, in Clusters of Galaxies: Probes of Cosmological Structure and Galaxy Evolution ed. J. S. Mulchaey, A. Dressler, & A. Oemler (Cambridge: Cambridge Univ Press), preprint (astro-ph/0305512)
- Mihos, J. C., Harding, P., Feldmeier, J., & Morrison, H. 2005, ApJ, 631, L41
- Moore, B., Katz, N., Lake, G., Dressler, A., & Oemler, A. 1996, Nature, 379, 613
- Murphy, E. J., Kenney, J. D. P., Helou, G., Chung, A., Howell, J. H. 2009, ApJ, 694, 1435
- Nulsen, P. E. J. 1982, MNRAS, 198, 1007
- Oosterloo, T., & van Gorkom, J. 2005, A&A, 437, L19
- Paturel, G., et al. 1997, A&AS, 124, 109
- Phillips, M. M., & Malin, D. F. 1982, MNRAS, 199, 205
- Phookun, B., Vogel, S. N., Mundy, L. G. 1993, ApJ, 418, 113
- Phookun, B., & Mundy, L. G. 1995, ApJ, 453, 154
- Rodgers, A. W., & Freeman, K. C. 1970, ApJ, 161, L109
- Sanchis, T., Solanes, J. M., Salvador-Solé, E., Fouqué, P., & Manrique, A. 2002, ApJ, 580, 164
- Sancisi, R., Thonnard, N., & Ekers, R. D. 1987, ApJ315, L39
- Schindler, S., Binggeli, B., & Böhringer 1999, A&A, 343, 420
- Schweizer, F., & Seitzer, P. 1992, AJ, 104, 1039
- Shibata, R., Matsushita, K., Yamasaki, N. Y., Ohashi, T., Ishida, M., Kikuchi, K., Böhringer, H., Matsumoto, H. 2001, ApJ, 549, 228
- Skrutskie, M. F., et al. 2006, AJ, 131, 1163
- Smith, R. J., Lucey, J. R., Hudson, M. J., Schlegel, D. J., Davies, R. L. 2000, MNRAS, 313, 469
- Solanes, J. M., Manrique, A., García-Gómez, C., González-Casas, G., Giovanelli, G., & Haynes, M. P. 2001, ApJ, 548, 97
- Solanes, J. M., Sanchis, T., Salvador-Solé, E., Giolvanelli, R., & Haynes, M. 2002, AJ, 124, 2440
- Spiegel, D. N., et al. 2003, ApJS, 148, 175
- Stauffer, J. R., Kenney, J. D., & Young, J. S. 1986, AJ, 91, 1286
- Taylor, G. B., Ulvestad, J. S., & Perley, R. A. 2004, The Very Large Array Observational Status Summary
- Tonnesen, S., Bryan, G. L., van Gorkom, J. H. 2007 ApJ, 671, 1434
- Tonnesen, S., & Bryan, G. L. 2008, 684, 9L
- Tully, R. B., & Shaya, E. J. 1984, ApJ, 281, 31
- Veilleux, S., Bland-Hawthorn, J., Cecil, G., Tully, R. B., & Miller, S. T. 1999, ApJ, 520, 111
- Vollmer, B., Cayatte, V., Boselli, A., Balkowski, C., & Duschl, W. J. 1999, A&A, 349, 411
- Vollmer, B. 2003, A&A, 398, 525
- Vollmer, B., Balkowski, C., Cayatte, V., van Driel, W., & Huchtmeier, W. 2004a, A&A, 419, 35
- Vollmer, B., Beck, R., Kenney, J. D. P., & van Gorkom, J. H. 2004b, AJ, 127, 3375
- Vollmer, B., Huchtmeier, W., & van Driel, W. 2005, A&A, 439, 921
- Vollmer, B., Soida, M., Otmianowska-Mazur, K., Kenney, J. D. P., van Gorkom, J. H., Beck, R. 2006, A&A, 453, 883
- Vollmer, B., Soida, M., Beck, R. et al. 2007, A&A, 464, L37
- Vollmer, B., Soida, M., Chung, A. et al. 2008, A&A, 483, 89
- Warmels, R. 1988a, A&AS, 72, 19
- Warmels, R. 1988b, A&AS, 72, 57
- West, M. J., & Blakeslee, J. P. 2000, ApJ, 543, L27
- Wezgowiec, M., Urbanik, M., Vollmer, B., Beck, R., Chyzy, K. T., Soida, M., Balkowski, C. 2007, A&A, 471, 93
- Wyder, T. K., Dolphin, A. E., & Hodge, P. W. 1998, MNRAS, 298, 259
- Yasuda, N., Fukugita, M., & Okamura, S. 1997, ApJS, 108, 417
- Yoshida, M., et al. 2002, ApJ, 567, 118